Phylogenomics of the psychoactive mushroom genus *Psilocybe* and evolution of the psilocybin biosynthetic gene cluster

*Alexander J Bradshaw[1,2], *Virginia Ramírez-Cruz[3], Ali R. Awan[4], Giuliana Furci[5], Laura Guzmán-Dávalos [6], Paul Stamets[7] , Bryn T.M. Dentinger [1,2]

[1]School of Biological Sciences, University of Utah, 201 Presidents Circle, Salt Lake City UT 84112
[2]Natural History Museum of Utah, University of Utah, 301 Wakara Way, Salt Lake City UT 84108
[3] CONACYT-Departamento de Botánica y Zoología, Universidad de Guadalajara, Apdo. Postal 1–139, Zapopan, 45147, Jalisco, Mexico
[4]Genomics Innovation Unit, Guy's and St. Thomas' NHS Foundation Trust
[5] Fungi Foundation, 716 Marcy Ave, Brooklyn, NY 11216, USA
[6]Departamento de Botánica y Zoología, Universidad de Guadalajara, Apdo. Postal 1–139, Zapopan, 45147, Jalisco, Mexico
[7]Fungi Perfecti LLC Laboratories, Shelton, Washington, USA

* These authors contributed equally to this work
Corresponding author: Alexander J Bradshaw

Abstract:

Psychoactive mushrooms in the genus *Psilocybe* have immense cultural value and have been used for centuries in Mesoamerica. Despite a recent surge in interest in these mushrooms due to emerging evidence that psilocybin, the main psychoactive compound, is a promising therapeutic for a variety of mental illnesses, their phylogeny and taxonomy remain substantially incomplete. Moreover, the recent elucidation of the psilocybin biosynthetic gene cluster is known for only five species of *Psilocybe*, four of which belong to only one of two major clades. We set out to improve the phylogeny for *Psilocybe* using shotgun sequencing of 71 fungarium specimens, including 23 types, and conducting phylogenomic analysis using 2,983 single-copy gene families to generate a fully supported phylogeny. Molecular clock analysis suggests the stem lineage arose ~66 mya and diversified ~53 mya. We also show that psilocybin biosynthesis first arose in *Psilocybe*, with 4–5 possible horizontal transfers to other mushrooms between 40 and 22 mya.

Moreover, predicted orthologs of the psilocybin biosynthetic genes revealed two distinct gene orders within the cluster that corresponds to a deep split within the genus, possibly consistent with the independent acquisition of the cluster. This novel insight may predict differences in chemistry between the two major clades of the genus, providing further resources for the development of novel therapeutics.

Introduction:

Members of the renowned psychoactive genus *Psilocybe* (Fr.) P. Kumm., colloquially known as "magic mushrooms," have become a major scientific and public curiosity since Robert Gordon Wasson first published his infamous *Life* magazine piece "Seeking the Magic Mushroom" in 1957 (Wasson 1957). *Psilocybe* sensu lato is a globally distributed genus of psychoactive mushrooms and in its traditional concept contains between 277 and 326 known species (Guzmán 2005; Kirk et al. 2008). Molecular phylogenetic studies have demonstrated that *Psilocybe* s.l. is not monophyletic (Moncalvo et al. 2002; Matheny et al. 2006). One group consists of species that exhibit a "bluing" reaction when damaged, a feature that is thought to indicate the presence of the psychoactive alkaloid psilocybin (Guzmán 2005; Lenz et al. 2020, 2021). However, only 24 of ~144 species with the bluing reaction have been included in multi-locus molecular phylogenetic datasets (Borovička et al. 2011; Ramírez-Cruz et al. 2013a).

While taxonomy of *Psilocybe* has been the subject of a handful of studies spanning the past 60+ years (Singer and Smith 1958; Hofmann et al. 1959; Guzmán 1983, 1995, 2005; Borovička et al. 2011; Ramírez-Cruz et al. 2013b; Cortés-Pérez et al. 2020), the ambiguous legal status of *Psilocybe* specimens and their rampant misidentification has hindered modern taxonomic research on them (Bradshaw et al. 2022). The only multi-locus molecular phylogenetic studies included 24 (accounting for found synonyms) species and up to three gene regions, with many branches without strong statistical support and lacking most of the currently recognized species (Borovička et al. 2011, 2015; Ramírez-Cruz 2013a). Moreover, most of the available molecular data do not come from type specimens, making it impossible to authenticate modern material. Together, our poor phylogenetic understanding and uncertainty in the application of names limit our ability to investigate evolutionary questions in *Psilocybe* and

impair the construction of a robust predictive framework for exploring genetic traits of potential interest for the development of novel therapeutics.

The enzymatic synthesis of the psychoactive compound psilocybin was first elucidated in *Psilocybe cubensis* (Earle) Singer and *P. serbica* M.M. Moser & E. Horak (Fricke et al. 2017). Four core genes encoding enzymes that convert the amino acid tryptophan into psilocybin occur in a cluster: PsiD (tryptophan decarboxylase), PsiK (kinase), PsiM (methyltransferase), and PsiH (P_{450}) (Fricke et al. 2017). Phylogenetic analysis indicated that this cluster has been horizontally acquired by psilocybin-producing mushrooms in other genera with common ecological niches (Awan et al. 2018; Reynolds et al. 2018), although the direction and relative timing of these transfers remains unclear. Notably, only a select few species of *Psilocybe* have been investigated at a genomic scale (Fricke et al. 2017; Awan et al. 2018; Reynolds et al. 2018; McKernan et al. 2021; Dörner et al. 2022), which does not represent all of the known ecologies, and they do not span the phylogenetic range of the two major clades identified by Ramírez-Cruz et al. (2013a), severely limiting inferences of evolutionary patterns.

Due to their relatively small genomes, whole genome sequencing of Fungi has been advancing at an expedited pace (Grigoriev et al. 2014). One of the major challenges to fungal molecular systematics has been the lack of available material due to the unpredictable and ephemeral nature of fungal reproductive structures, and the poor preservation of DNA in fungarium specimens. However, the technical impediment to utilizing preserved specimens has been largely overcome and it is now feasible and relatively cost-effective to generate whole metagenomes from fungarium specimens for phylogenomics (Dentinger et al. 2016 Tremble et al. 2020, Liimatainen et al. 2022). In this study, we aimed to vastly improve our understanding of *Psilocybe* evolution by increasing the species represented in a genome-scale phylogenetic dataset

by exploiting fungarium resources and using the phylogeny as a backbone constraint to incorporate all publicly available DNA sequence data for *Psilocybe* and to explore the evolution of psilocybin biosynthesis.

Results:

Sequencing and genome assembly:

Genomic DNA (gDNA) libraries were prepared using Nextera DNA Flex Library Prep and sequenced using Novaseq 2x 150bp. Total reads for samples ranged from 3,909,488 reads (Psilocybe_mexicana_IBUG-13593, ~11.7x coverage) to 225,748,454 reads (Psilocybe_baeocystis_WTU-F-011245, ~ 677.2x coverage). Across all of our samples, we achieved an average of 94,490,694 reads (~283.5x coverage) and a median of 99,070,482 reads (~297.2x coverage).

Following genome assembly, statistics for each sample were measured with N50 values ranging from 554 (Psilocybe_tuberosa_WTU-F-011378) to 60,042 (Psilocybe_stuntzii_WTU-F-011520) and the number of contigs for each assembly ranging from 7,004 (Psilocybe_stuntzii_WTU-F-011520) to 784,732 (Psilocybe_caerulescens_var_mazatecorum_SFSU-F-029971). It should be noted that these assemblies are likely to be highly non-contiguous due to the fact they are from museum vouchers, which are susceptible to high amounts of contamination and should be treated as metagenome assemblies (Dentinger et al. 2016).

In addition to looking at assembly statistics, we compared the recovery of single-copy orthologs based on the agaricales_odb10 reference database to judge the “completeness” of our genomes. We observed BUSCO scores ranging from 30.7% (Psilocybe_fuliginosa_NY-

1901148) to 95.4% (Psilocybe_stuntzii_WTU-F-011520). In terms of complete BUSCO gene recovery, only one sample achieved a score of ~95% (the general measurement of a high-quality assembly), yet phylogenomic data utilizing museum vouchers have been shown to allow for robust generation of phylogenetic relationships with strong support values, especially those at deeper nodes, which are often difficult to resolve (Dentinger et al. 2016) All assembly statistics and BUSCO scores for each sample are reported in Supplementary Table 1.

Psilocybe phylogenomic species tree and divergence time of major clades:

Specimens of *Psilocybe* were selected based on species-level voucher designation and totaled 71 specimens, 23 of which were type specimens, the ultimate name-bearing specimen for a species (Aime et al. 2021) (Table 1). Of the 71 specimens, 52 were true *Psilocybe* (*Psilocybe* sensu stricto) (20 type specimens) (Figure 1), 19 were found to not be true *Psilocybe*: 14 specimens clustered together phylogenetically, and belonged to *Deconica* (W.G. Sm.) P. Karst. (*Psilocybe* sensu lato) (3 type specimens), 3 clustered together, only identifiable to *Strophariaceae*, one specimen was found to b*e Kuehneromyces* sp. (Psilocybe_laticystis_UBC-F16759), and one sample was unable to be accurately identified (Psilocybe_washingtonensis_WTU-F-055019) and was removed from the further downstream analysis (Supplementary Figure 1, Table1).

Phylogenomic analysis using our specimens and six outgroup taxa was performed with a profile of 2983 single-copy genes derived from MCL (Markov Cluster Algorithm) clustering (Psiser 1 comparative clustering .2497) generated through MycoCosm. Two methods were used: the first was the concatenation of genes into a single supermatrix for analysis (Supplementary Figure 1). The second was a summary coalescent model of all 2983 gene trees (Supplementary

Figure 2). Both trees were topologically congruent and exhibited excellent nodal support in nearly all branches. Our species tree generated two major clades that match clade I and clade II previously reported in Ramírez-Cruz et al. (2013a), but included the representation of 39 new species, which had not been investigated in that study (Figure 2, left).

To investigate the splitting of these major clades further, we performed molecular dating using two separate methods with calibration points set between 57 and 71 mya to represent the divergence of the family *Hymenogastraceae* (to which *Psilocybe* belongs). The first method utilized uncorrelated penalized likelihood with a "relaxed" molecular clock model, which assigned the most recent common ancestral node for clade I and clade II an age of 64.2 mya. The second method used was the estimation of divergence dates in the absence of a molecular clock through r8s (Sanderson 2003), which assigned the most recent common ancestral node for clade I and clade II an age of 60.5 mya.

Phylogenetic analysis of ITS, EF1a, RPB1, and RPB2 genes, and macro-and micromorphology for specimen misidentification:

In addition to phylogenomics, we chose to extract the universal fungal barcode, ITS (Schoch et al. 2012), and the common phylogenetic single-copy protein-coding genes elongation factor 1-alpha (EF1a), the largest subunit of RNA polymerase II (RPB1), and the second-largest subunit of RNA polymerase II (RPB2)(Supplementary Figures 3–6). We did this to rationalize our dataset with publicly available data to provide the most accurate representation of *Psilocybe* possible. Across all publicly available sequences, 40 unique taxonomic names were represented, ~13% of the approximately 150 currently accepted *Psilocybe* s.s. However, sequence number

and taxonomic representation of molecular markers varied widely. No species retrieved from the public databases had all gene regions representing a single voucher specimen. In total, the analysis of sequences from the public database along with markers extracted from our genome assemblies provided a representation of 67 unique taxa, 17 of which were represented only in the public databases. In comparison, our data set provided sequence representation for 27 taxa not previously reported. In particular, the inclusion of public data was vital for our work as it allowed us to pinpoint specimens that are likely misidentified at the species level, a common issue in museum fungaria and *Psilocybe* in particular (Figure 2, Table 1) (Andrew et al. 2019; Bradshaw et al. 2022).

While the representation of sequences for the markers was modest (EF1a n=32, RPB1 n=30, RPB2 n=15, and ITS n=26), the addition of these sequences to our phylogenomic tree enabled us to add representation for six species from EF1a, nine from RPB1, three from RPB2, and 11 from ITS for which we did not have specimens. In all gene trees, four specimen vouchers were consistently incongruent with the other taxa they clustered with: "*Psilocybe acutissima*" (GAM-00011063), "*Psilocybe baeocystis*" (WTU-F-011245), "*Psilocybe quebecensis*" (NY-1901130), and "*Psilocybe silvatica*" (VPI-F-0003693) (Supplementary Figures 3–6). These specimens were then further analyzed using macro- and micromorphological traits to confirm that they were indeed misidentified vouchers. From the comparison of macro- and microscopic features, it was determined that GAM00011063 was mostly likely *Psilocybe hoogshagenii* R. Heim, VPI-F-003693 and NY-1901130 were mostly likely *Psilocybe caerulipes*, while WTU-F-011245 was mostly likely *Psilocybe cyanescens* Sacc..

New combinations in *Deconica*:

Based on genomic data of type specimens, three new combinations in *Deconica* are proposed for those species that formerly were described as *Psilocybe*, in order to use the correct name.

Deconica subpsilocybioides (Guzmán, Lodge & S.A. Cantrell) Bradshaw, Ram.-Cruz & Dentinger, **comb. nov.**

MycoBank no.:489154

Index Fungorum Registration Identifier 489154

Basionym. – *Psilocybe subpsilocybioides* Guzmán, Lodge & S.A. Cantrell, in Guzmán, Tapia, Ramírez-Guillén, Baroni, Lodge, Cantrell & Nieves-Rivera, Mycologia 95(6): 1174 (2003)

Deconica clavata (Guzmán) Bradshaw, Ram.-Cruz & Dentinger, **comb. nov.**

MycoBank no.:109209

Index Fungorum Registration Identifier 109209

Basionym. – *Psilocybe clavata* Guzmán [as 'clavatum'], Beih. Nova Hedwigia 74: 307 (1983)

Deconica lazoi (Singer) Bradshaw, Ram.-Cruz & Dentinger, **comb. nov.**

MycoBank no.:337850

Index Fungorum Registration Identifier 337850

Basionym. – *Psilocybe lazoi* Singer, Beih. Nova Hedwigia 29: 242 (1969)

Evolution of the psilocybin-producing gene cluster within *Psilocybe*:

Gene prediction using Augustus and a reciprocal best blast (RBB) hit method were used to extract and confirm each of the core gene sequences (PsiD, PsiK, PsiM, and PsiH). Identifications were compared to gene prediction output to determine the order and orientation of each gene in the cluster based on the strand position (+/-) of the start codon for each gene (Figure 2, center). In addition to Augustus and RBB, we also utilized Exonerates protein2genome function to confirm our results. In most cases, the gene predictions from Exonerate matched those from Augustus/RBB, with disagreements still having correct gene hits. In a few cases, we found that Exonerate identified genes more accurately and with less ambiguity compared to our RBB method (Supplementary Table 2).

We found variability in the order of the four core psilocybin-producing cluster genes within our expanded representation of *Psilocybe* species, identifying two distinct patterns. The first pattern followed a gene order of PsiD>PsiM,>PsiH>PsiK, the canonical gene order originally reported from *Psilocybe cubensis* and *Psilocybe serbica*, and was represented entirely by clade II of our dataset. The second was PsiD>PsiK>PsiH>PsiM, found in clade I of our species tree (Figure 2, right). Across our phylogeny, the original pattern was represented by 17 *Psilocybe* specimens, while 35 of our *Psilocybe* specimens exhibited the newly identified pattern.

In addition to gene order and orientation, we investigated the molecular sequence evolution of each gene separately. Phylogenetic analysis was performed without using our species constraint tree for each core psilocybin-producing genes, PsiD, PsiK, PsiM, and PsiH (Figure 2, right). We found that PsiD, PsiK, and PsiM all had the same sample clustering and topology as our species tree, suggesting a vertical inheritance pattern for these genes in *Psilocybe*. However, the gene tree for PsiH had clustering patterns consistent with our species tree but an incongruent topology, with clade II derived within clade I PsiH, rendering clade I

PsiH paraphyletic. We found PsiH was far more diverse than the other core genes upon more in-depth investigation, with a much larger number of similar genes. Further, multiple samples, primarily from clade II, were found to have multiple copies of PsiH from our gene predictions (Figure 2, right, and Supplementary Table 2).

Psilocybin homologs genes present outside of *Psilocybe* and ecological niche patterns:

In contrast to only looking at the molecular evolution of the psilocybin gene cluster within *Psilocybe*, we investigated the known horizontal gene transfer (HGT) events from *Panaeolus* (Fr.) Quél., *Gymnopilus* P. Karst., and *Pluteus* Fr., using publicly available data and newly sequenced specimens vouchered as *Gymnopilus luteofolius* (Peck) Singer, *Pluteus albostipitatus* (Dennis) Singer, and *Pluteus salicinus* (Pers.) P. Kumm (Table 1 and Figure 3, left). Gene prediction and RBB analysis yielded representation of the four core psilocybin-producing genes from the published genomes of *Panaeolus cyanescens* and *Gymnopilus dilepis* (Berk. & Broome) Singer, and our newly sequenced *Gymnopilus luteofolius* and *Pluteus salicinus* genomes (Supplementary Table 2).

Phylogenetic analysis of the PsiD gene, including those from our *Psilocybe* genomic samples, and publicly available sequences, revealed three branching patterns for our non-*Psilocybe* taxa. The first branch contained *Conocybe smithii* Watling (= *Pholiotina smithii* (Watling) Enderle) as a monophyletic branch sister to our *Psilocybe caerulipes* (Peck) Sacc. samples (BS 100%). The second branch placed *Panaeolus cyanescens* as a sister group to *Psilocybe cubensis* (BS 100%), and the final contained species of both *Gymnopilus* and *Pluteus* sharing a most recent common ancestor with all of *Psilocybe* (BS 100%) (Figure 3, left).

After expanding *Psilocybe* diversity and refining the placement of known HGT events, we sought to identify whether phylogenetic clusters could be attributed to specific ecological niches. Interestingly, our two primary phylogenetic clades correspond to distinct ecological lifestyles, with a few notable exceptions (Figure 3, left). The clade I cluster, identified through our PsiD analysis, corresponds almost entirely to the soil-dwelling saprotrophic lifestyle, except for the *Psilocybe caerulipes* grouping, which exhibits wood decay (i.e., rotting wood rather than soil enriched with woody debris) ecology. *Psilocybe* Clade II, *Gymnopilus* and *Pluteus* were associated primarily with wood decay, and in the case of *Psilocybe cubensis* and *Panaeolus cyanescens*, a coprophilous lifestyle (Figure 3, left).

Divergence times of taxa known to produce psilocybin compared to the molecular evolution of the decarboxylase (PsiD) gene:

To further investigate the evolutionary history of psilocybin acquisition, we performed a phylogenetic analysis of taxa known to contain the psilocybin gene cluster. We utilized the large ribosomal subunit (LSU) for analysis as it had the greatest diversity representation from public resources across all the taxa studied, compared to other standard protein-coding markers such as EF1a, RPB1, and RPB2. In our analysis, we targeted six specific points of psilocybin production: 1) emergence of the *Psilocybe* genus, 2) presence in *Pluteus*, 3–4) acquisitions within *Panaeolus*, 5) acquisition in *Conocybe* Fayod/*Pholiotina* Fayod, and 6) presence within *Gymnopilus* (Figure 3, right). Divergence dating of these taxa suggests that *Psilocybe* is the oldest lineage to produce psilocybin, having diverged between ~50 mya and ~68 mya, similar to the divergence times observed from our phylogenomic dataset of ~65 mya. Next, presence in *Pluteus* emerged

between ~40 mya and ~53 mya. In *Panaeolus*, phylogenetic analysis showed two, possibly individual, acquisitions for *Panaeolus cyanescens* and *P. subbalteatu*s occurring between ~15-21 mya and ~25-43 mya, respectively. Further, acquisition in *Conocybe*/*Pholiotina* seems to have happened between ~26 mya and ~36 mya, and finally the most recent emergence in *Gymnopilus* between ~6 and 9 mya (Supplementary Table 3).

Comparison of the taxonomic relationship of *Psilocybe* and non-*Psilocybe* psilocybin producing taxa to the molecular evolution of PsiD for these same groups reveals that psilocybin likely emerged first in *Psilocybe*, which has passed the gene cluster to *Panaeolus* and *Conocybe*/*Pholiotina*. However, PsiD genes for both *Gymnopilus* and *Pluteus* are more closely related to one another than to *Psilocybe*. The emergence of psilocybin production in *Pluteus* occurs 30-40 my before the presence in *Gymnopilus* suggesting possible transfer from *Pluteus* to *Gymnopilus*, but more diverse representation in both groups would be needed to further refine this pattern.

Discussion:

Phylogenomics of *Psilocybe*

Our phylogenomic analysis of 2,983 single-copy genes resulted in a single, unambiguous and statistically supported phylogeny for 52 species of *Psilocybe* s.s. This more than doubles the number of species included in previous analyses. Our focus on generating whole genomes from types, as old as 65 y, provided unequivocal placement of known species and a rich resource for authentication of modern and future samples. The perfect congruence of the topologies inferred from a partitioned supermatrix analysis and a summary coalescent of individual gene trees is strong evidence that the inferred phylogeny is robust to methodological approach. Because we

294 utilized whole genome sequencing instead of reduced representation markers, this allowed us to
295 explore genomic patterns within a robust phylogenetic context, illuminating a novel phylogenetic
296 dichotomy in the arrangement of the genes that make up the psilocybin biosynthetic gene cluster
297 (BGC). This dichotomy aligns with a deep divergence within the genus around 53 mya,
298 providing new insights into the evolutionary history of this enigmatic and iconic natural product
299 and a resource for potential development of new therapeutics.
300 Our phylogeny has nearly perfect (100%) nodal support at every branch (Fig. 1),
301 including deeper branches within the backbone that are often difficult to resolve in mushrooms
302 (Dentinger et al. 2016, 2016; Matheny et al. 2006; Moncalvo et al. 2000, 2002). The two main
303 clades within *Psilocybe* as reported by Ramírez-Cruz et al. (2013a) were also recovered here,
304 indicating an early split within the genus that coincides with the genic arrangement of the
305 psilocybin BGC, but precedes a shift in ecology. Our results suggest that *Psilocybe* arose as
306 primarily a wood-decomposing group that transitioned to soil after the split, with two shifts to
307 dung-decomposition. However, critical species, such as the African dung-dwelling *P. natalensis*
308 Gartz, D.A. Reid, M.T. Sm. & Eicker, are still missing, which may have an impact on the
309 patterns seen here.
310
311 New insights on *Psilocybe* taxonomy
312 The inclusion of taxa that had not been previously sampled reveals new infrageneric
313 divisions of *Psilocybe* that contradict morphological-based classifications. For example, our
314 results show that *P. aztecorum* R. Heim is sister to the *P. serbica* complex (sect. *Semilanceatae*
315 Guzmán) rather than *P. baeocystis* in sect. *Aztecorum* Guzmán (1983). Together this group
316 occupies a strictly temperate distribution in Europe, the USA, and high elevations of central

Mexico. Also, the addition of the isotypes of *P. guilartensis* Guzmán, F. Tapia & Nieves-Riv., *P. heimii* Guzmán, *P. pleurocystidiosa* Guzmán, and *P. singeri* Guzmán, (sect. *Brunneocystidiatae* Guzmán), all belong to an expanded "cordisporae" clade. All of these species have rhomboid basidiospores (heart-shaped and hence the term "cordisporae") and yellowish basal mycelia, confirming the morphological cohesion first proposed by Ramírez-Cruz et al. (2013a). The "zapotecorum" clade was also expanded to include *P. angustipleurocystidiata* Singer & A.H. Sm., *P. argentipes* K. Yokoy. (=*P. subcaerulipes* Hongo), *P. columbiana* Guzmán, and *P. hoogshagenii* var. *convexa* Guzmán. All of these taxa have small, ellipsoid or subrhomboid basidiospores, but otherwise unifying morphological characteristics are unknown.

Our results also provide new insights into well-known species complexes. For example, the species complex surrounding the European *P. moravica* Borov. (consisting of *P. arcana* Borov. & Hlaváček, *P. bohemica* Šebek, *P. moravica*, and *P. serbica*) were extremely similar with two separate clustering patterns (*P. arcana*/*P. moravica* and *P. serbica*/*P. bohemica*)(Figure 2). This strongly implies they are all part of a single, variable species as proposed by Borovička et al. (2011), or undergoing rapid diversification. Similarly, *P. semilanceata* (Fr.) P. Kumm. clustered with *P. liniformans* var. *americana* Guzmán & Bas, sister to *P. callosa* (Fr.) Gillet and *P. subfimetaria* Guzmán & A.H. Sm. Although none of these were derived from types, this suggests that *P. liniformans* var. *americana* is synonymous with *P. semilanceata*, which is very close to *P. callosa* and *P. subfimetaria* (which may also be conspecific). Our results are also inconsistent with synonymies based only on morphological features. Cortés-Pérez et al. (2020) synonymized *P. weilii* Guzmán, Stamets & F. Tapia and *P. wrightii* Guzmán with *P. caerulescens* Murrill, whereas our results indicate there are substantial genetic differences between them and there is a strong possibility that, in fact, they represent distinct species.

Two very similar species, *Psilocybe cubensis* and *P. subcubensis* Guzmán, have variably been treated as one or two species. *Psilocybe subcubensis* was first segregated from *P. cubensis* in 1978 based on its smaller basidiospores and more tropical distribution (Guzmán and Vergeer 1978; Guzmán 1983). Both taxa form a species complex with very few diverging phenotypic differences between them (Alban-J. et al. 2021; Chethana et al. 2021). However, our data show a well-supported (BS 99%) split between groupings of *P. cubensis* and *P. subcubensis*, albeit with very short branches, suggesting that *P. subcubensis* is not conspecific with *P. cubensis*. The difference in spore size between these two taxa is possibly an early example of a morphological trait that indicates species divergence within the *P. cubensis* species complex.

Evolution of *Psilocybe cubensis*

Interestingly, the branch leading to *P. cubensis/subcubensis* (sect. *Cubensae* sensu Guzmán 1983) is longer than expected for recently diverged taxa (Parks and Goldman 2014), suggesting that additional closely related taxa are missing (Ramírez-Cruz et al. 2013a) or the lineage has experienced accelerated evolution. Guzmán (1983) predicted that *P. cubensis*, a cow and horse-dung specialist originally described from Cuba by Earle in 1909, was brought to the Americas from Africa by the Spanish. Thus, it is possible that *P. cubensis* is a "self-domesticated" species that has undergone parallel evolution during the domestication of cattle. Although *P. cubensis* has not been officially reported from Africa, Guzmán predicted that other species close to it remain to be discovered there. The only African species included in a phylogenetic dataset is the *P. congolensis* Guzmán, S.C. Nixon & Cortés-Pérez we included, which is not closely related to *P. cubensis* (Figure 2). In contrast, Ramírez-Cruz et al. (2013a) reported that the sister taxon to *P. cubensis* is *P. thaiaerugineomaculans* Guzmán, Karun. &

Ram.-Guill. from Thailand, which we also recovered in our RPB1 tree (Supplementary Figure 5). We additionally recovered *P. chuxiongensis* T. Ma & H.D. Hyde from Yunnan, China (Ma et al. 2014) as a sister taxon to *P. cubensis* in our ITS tree (Supplementary Figure 3. These results suggest an Asian rather than African origin for the progenitor of *P. cubensis*. However, sequences labeled as *P. natalensis* (KwaZulu-Natal, South Africa) deposited in NCBI do show close relationships with *P. cubensis* (Bradshaw et al. 2022), although these sequences do not have voucher information included, rendering them dubious. Nonetheless, these results align with African *Psilocybe* assigned morphologically to the Cubensae complex by Froese et al. (2016). Inclusion of types of the African species as well as new, targeted fieldwork is needed to clarify the relationship of *P. cubensis* and provide clearer insight into its origin.

Evolution of the psilocybin biosynthetic gene cluster within *Psilocybe*

Our results are consistent with a strictly vertical inheritance pattern of the psilocybin BGC within *Psilocybe*. However, the two distinct gene order patterns correlate with a deep divergence within the genus approximately 53 mya. While it is unclear what the origin of these two patterns is, the early divergence and subsequent maintenance of the gene orders within the two clades may indicate additional variation early in the evolution of the psilocybin BGC. Such variation may have existed in the nascent stages of psilocybin biosynthesis, possibly in response to selective forces acting to shape its function. This discovery also indicates that transcriptional regulation of the genes may vary among taxa, resulting in taxon-specific metabolic profiles (Hoffmeister and Keller 2007; Yin and Keller 2011). Such knowledge could be harnessed in future bioengineering work to optimize and customize psilocybin biosynthesis, or as yet unknown analogs, in heterologous systems.

386

387 Duplication of PsiH

388 Upon deeper investigation of PsiH, we found that it had considerably more sequence
389 variation than any of the other core genes and has undergone multiple duplications or multiple
390 losses (Figure 2, Supplementary Table 2). However, upon adding second best hit identified
391 duplicated sequences similar to PsiH gene predictions, we found that the splitting of clade II
392 became less severe, suggesting multiple paralogs across are present in many species of
393 *Psilocybe*, despite having bioinformatically reducing our genomes to haploid values. These
394 findings may be of particular importance for future uses in the pharmaceutical production of
395 these compounds by providing multiple options of genes for optimizing the expression and
396 production in organisms such as *Escherichia coli* Escherich and *Saccharomyces cerevisiae*
397 (Desm.) Meyen (Adams et al. 2019; Milne et al. 2020).

398 While we primarily found duplications to occur in clade II taxa, we do not rule out that
399 this pattern is far more pervasive across the genus. We utilized a sliding window analysis to
400 build the most consecutive cluster placement possible. Due to this methodology, we can
401 confidently report cluster gene order and orientation when genes were assembled within the
402 same contig; however, this method does not perform as well on samples with more discontiguous
403 assemblies, which is a hallmark of metagenomic assemblies from museum specimens. While this
404 is the largest dataset of this kind in *Psilocybe*, future studies should place considerable effort on
405 re-collecting and sequencing highly contiguous genomes of these specimens to continue to
406 expand our repertoire of questions in *Psilocybe*.

407

408 Patterns of inheritance and relative timing of psilocybin biosynthesis

Psilocybin and psilocin production has been reported in taxa evolutionarily distant from *Psilocybe*, including *Conocybe/Pholiotina*, *Gymnopilus*, *Inocybe* (Fr.) Fr., *Panaeolus*, and *Pluteus* (Christiansen et al. 1984; Gartz 1987; Guzmán et al. 1998; Awan et al. 2018). Reynolds et al. (2018) and Awan et al. (2018) showed that the psilocybin BGC was horizontally acquired in *Conocybe/Pholiotina*, *Gymnopilus*, *Panaeolus*, and *Pluteus*, but the direction and relative timing remained ambiguous. Using a secondary calibration from He et al. (2019) for the origin of Agaricales, our results show that psilocybin biosynthesis was first acquired by *Psilocybe* around 65 mya and was acquired by *Conocybe/Pholiotina*, *Gymnopilus*, *Panaeolus*, and *Pluteus* in multiple events between 44–7 mya (Figure 3, right).

In our analysis of the PsiD gene, we identified two clear HGT events from *Psilocybe* to other genera consistent with Reynolds et al. (2018) (Fig. 3): 1) *Conocybe smithii* (= *Pholiotina smithii*) is nested within *Psilocybe*, sharing a most recent common ancestor with the *Psilocybe caerulipes* complex, and 2) *Panaeolus cyanescens* is recovered sister to *Psilocybe cubensis*. However, *Gymnopilus* and *Pluteus* PsiD are not nested within *Psilocybe* (Figure 3, right). Such a pattern is inconsistent with HGT from *Psilocybe*, especially given the chronology of psilocybin evolution (Figure 3, right). Instead, the phylogeny indicates that the psilocybin BGC may have been acquired independently by *Gymnopilus*, *Pluteus*, and *Psilocybe*, from an as yet unidentified source or multiple sources. Reynolds et al. (2018) speculated that the psilocybin BGC may have originated in *Fibularhizoctonia* G.C. Adams & Kropp, a genus of anamorphic *Athelia* Pers. that has multiple copies of Psi homologs, albeit not contained in a cluster (Konkel et al. 2021). The Atheliales are close relatives of the Agaricales with a broad range of ecologies, including termite symbionts (Matsuura 2005), plant pathogens, mycorrhizal mutualists, and saprobes. Reynolds et al. (2018) speculated that this insect association may have provided the selective force for the

evolution of psilocybin as a modulator of the symbiosis. Interestingly, *Athelia arachnoidea* (Berk.) Jülich is mycoparasitic on lichens common on tree bark in north temperate regions (Arvidsson 1976, 1978), whereas its anamorph *Fibularhizoctonia carotae* (Rader) G.C. Adams & Kropp is pathogenic on carrot roots (Adams & Kropp 1996). Our results suggest wood decomposition as the ancestral ecology of *Psilocybe*, and both *Gymnopilus* and *Pluteus* are wood decomposers. This correlation of wood as a substrate for these mushrooms and the mycoparasitic ecology of the teleomorphic *Athelia arachnoidea* on bark in shared habitats is intriguing. Mycoparasitism may be one way the psilocybin BGC could be transferred horizontally and could explain the multiple HGT events to *Gymnopilus*, *Pluteus*, and *Psilocybe* inferred from our Psi gene phylogenies and that occurred as long ago as 65 mya and as recently as 7 mya. However, *Psilocybe* spp. are not known to have mycoparasitic behaviors that would explain the clear HGT events to *Panaeolus* and *Conocybe*/*Pholiotina*. That does not mean that they do not, however, as this behavior has never been examined in *Psilocybe* and other mushrooms can exhibit dual mycoparasitic and saprotrophic ecologies (Caiafa and Smith 2022).

Insights into the functional role of psilocybin

Despite its prominence in the scientific and public imagination, the functional role of psilocybin remains an enigma. The prevailing explanation is that psilocybin functions as an insect antifungivory defense compound (Reynolds et al. 2018). However, this prevailing idea requires more investigation as psilocybin mushrooms are often reported to be occupied by insects laying eggs or living larvae in senesced field collections. Psilocybin is a prodrug that is rapidly converted to the dephorphorylated psilocin, which mimics serotonin and binds tightly to serotonin receptors, especially 5-HT_{2A}, a pharmacological action common to many psychoactive

tryptamines (Araújo et al. 2015). High-affinity binding to these receptors in mammals, and homologs in distantly related organisms such as insects and arachnids, produces unnatural and altered behaviors (Christiansen et al. 1962; Nichols et al. 2002; Passie et al. 2002; Boyce et al. 2019). This disorientation may be a direct deterrent or could render the subject more vulnerable to predation (or, alternatively, may be a reward). Serotonin receptors are also highly expressed in the lining of a wide range of animal gastrointestinal tracts where serotonin is involved in digestion (French et al. 2014). Thus, it is also possible that psilocybin functions as an emetic or laxative to promote the dispersal of spores before they are rendered inviable by digestion. However, other than humans, there are few documented cases of vertebrates consuming psilocybin-containing mushrooms (consisting entirely of domesticated dogs) (Beug et al. 2006), many of which are uncommon or scarce and would be difficult to learn to recognize with minimal encounters, limiting their selective potential. Moreover, anecdotes of larvae-infested *Psilocybe* abound and one experiment showed that adult flies could be reared from *P. cyanescens* mushrooms that were identical to flies reared from a co-occurring non-psilocybin containing mushroom (Awan et al. 2018). Experimental evidence for the functional role of psilocybin is thus far lacking.

Lenz et al. (2020) elucidated the chemical basis of the blue pigment that forms when psilocybin-containing mushrooms are damaged as oligo- and poly-mers of psilocin. The conversion of psilocybin to psilocin and the linking of them into chains is enzymatically controlled. Lenz et al. (2020) also pointed out that the psilocin oligo/polymers have chemical properties similar to plant flavonoids and polyphenolic tannins, which produce reactive oxygen molecules that can cause lesioning in the basic and oxidative environment of invertebrate guts. Thus, the psilocin oligo/polymers may be an inducible defense against fungivory, whereas

psilocybin may function simply as the building block kept in reserve for the true chemical weaponry. Intriguingly, the formation of the blue psilocin oligo/polymers is invariably connected to psilocybin biosynthesis throughout the multiple independent inheritances (Reynolds et al. 2018; Awan et al. 2018) and convergent evolution (Awan et al. 2018). The maintenance of the enzymatic capacity to inducibly convert psilocybin lends further support to the hypothesis that it is the blue oligo/polymer with an ecological function rather than the possibly accidental pharmacological effects of psilocybin, itself.

Although empirical evidence of inducible defenses against fungivory in mushrooms is largely lacking, one study demonstrated experimentally that the ubiquitous mushroom volatile 1-octen-3-ol is an inducible slug antifeedant (Wood et al. 2000). Interestingly, 1-octen-3-ol is also an insect attractant, including mosquitoes that are attracted to it in human breath and sweat (Takken and Kline 1989). Other fungivorous insects are also known to be attracted to 1-octen-3-ol including Culicoides (midges) and tsetse flies (Hall et al. 1984; Kline et al. 1994; Grant and Dickens 2011), suggesting that its recognition is likely fairly ancient as it would indicate food sources or brooding sites. In fact, 1-octen-3-ol is a critical element of the mushroom mimicry displayed by *Dracula* Luer orchids to attract pollinating *Zygothrica* Wiedemann flies (Joulain 1993; Kaiser 2006; Policha et al. 2016). The attractive quality of 1-octen-3-ol to insects and its ubiquitous presence in mushrooms are inconsistent with the hypothesis that insect fungivory has widespread negative impacts in mushrooms. However, the slug antifeedant property of 1-octen-3-ol suggests it may primarily function to stave off damage from fungivorous gastropods. Intriguingly, terrestrial gastropods first arose and diversified at the end of the Cretaceous mass extinction (Sohl 1987; Morris and Taylor 2000; Kaim 2002; Neubauer and Harzhauser 2022), concomitant with our inferred origin of psilocybin biosynthesis in *Psilocybe*. In contrast, insects

and angiosperms underwent evolutionary expansion during the Cretaceous from 145.5 and 65.5 mya, but suffered mass extinction following the impact of the asteroid that, by some estimates, caused nearly 80% of living species to go extinct (Raup and Boyajian 1988; Briggs 1991). Taken together, we hypothesize that psilocybin evolved as a pro-building block for an inducible chemical defense against fungivorous gastropods. Experimental studies will be critical to test this hypothesis.

Conclusion

Since the "re-discovery" of *Psilocybe*, this group of organisms and its unique psychoactivity has been of great interest from cultural, counter-cultural, scientific, and medical perspectives. However, *Psilocybe*, and the production of psilocybin and psilocin in general, hold numerous biological secrets that remain to be elucidated. Our study highlights how whole genome sequencing can enrich systematics studies by providing opportunities to examine patterns of gene evolution of a phenotypic trait. By mining genomic data beyond markers for phylogenetic inference, we gained novel insights into the evolutionary origins of psilocybin biosynthesis that have implications for understanding the functional role of this powerful chemical and can inform translational applications for human well-being.

Methods

DNA extraction and genomic sequencing

Sample tissue was extracted from the hymenophore ranging from 5–15 mg (our best extraction results usually came from large inputs between 10 and 15 mg).

These fragments were homogenized by placing them in 2.0 mL screw-cap tubes containing a single 3.0 mm and 8 1.5 mm stainless steel beads and shaking them in a BeadBugmicrotube homogenizer (#Z763713, Sigma) for 120 seconds at a speed setting 3500 rpm. DNA extraction was performed with NEB genomic monarch kit (monarch kit T3010S) with in-house protocol alterations to use the provided tissue lysis buffer at double volume and increase the amount of wash buffer to 550 µl during the washing steps.

Samples that had been collected before 1950 (such as many of the type specimens) were processed with a phenol-chloroform DNA extraction protocol. In short, mechanical disruption of tissue was followed as previously stated, then total lysate was placed in phase lock gel tubes (Quantabio #2302820) along with 1:1 volume of phenol/chloroform solution (Calibiochem OmniPur, EMD Millipore Corporation #5.39680.0002) and then mixed for 10 minutes on a hula mixer. Homogeneous mixtures were centrifuged at maximum speed for 10 minutes, then the aqueous (top) layer was transferred to a new phase-lock gel tube, and each step was repeated a second time before moving on. After extractions, precipitation was performed by ethanol precipitation with 7.5 molar ammonium acetate. gDNA samples were submitted to the High Throughput Genomics Core at the University of Utah, where libraries were prepared using Nextera DNA Flex Library Prep (cat: 20018704) and sequenced on a full lane of Novaseq 2× 150 bp.

Quality control and genome assembly

Sequencing run statistics and quality were visualized for each sample using Fastqc version 0.11.9 (CITATION?) and then compared to each other using MultiQC version 1.10 (Ewels et al. 2016). Library estimates were generated using the EstimateLibraryComplexity function of Picard toolkit

(http://broadinstitute.github.io/picard/), while genome assembly stats were quantified using a custom Perl script. Raw sequencing reads were trimmed and quality filtered using fastP version 0.20.1 (Chen et al. 2018) and then assembled using SPAdes version 3.15.2 (Bankevich et al. 2012) with kmer values alternating every other digit between 1 and 127, inclusive.

Homologous gene identification and phylogenetic species tree construction

Homologous genes used for phylogenetic analysis were identified by accessing publicly available MCL gene sequences from the Psiser1 comparative clustering.2497 profile (Fricke et al. 2017) through the Joint Genome Institute's (JGI) Mycocosm genome portal (Grigoriev et al. 2012, 2014). This profile included two species of *Psilocybe* (*P. cubensis* and *P. serbica*) (Fricke et al. 2017) and six closely related taxonomic outgroups, *Agrocybe pediades* (Fr.) Fayod (Agrped1) (Ruiz-Dueñas et al. 2021), *Galerina marginata* (Batsch) Kühner (Galma1) (Riley et al. 2014), *Gymnopilus chrysopellus* (Berk. & M.A. Curtis) Murrill (Gymch1), *G. junonius* (Fr.) P.D. Orton (Gymjun1) (Ruiz-Dueñas et al. 2021), *Hebeloma cylindrosporum* Romagn. (Hebcy2) (Mycorrhizal Genomics Initiative Consortium et al. 2015), and *Pholiota alnicola* (Fr.) Singer (=*Flammula alnicola* (Fr.) P. Kumm.)) (Phoaln1)(Ruiz-Dueñas et al. 2021), which contained 2,983 single-copy genes. While not the closest relative of *Psilocybe*, reference sequences for these 2,983 were taken from Galma1:v1 (*Galerina marginata*) (Riley et al. 2014) to facilitate a more conservative approach to homology identification in our sequenced genomes.

The Galma1 reference sequences were then used as a basis for the pairwise alignment tool Exonerate version 2.4.0 (Guy St.C. 2000) to extract representative sequences of each single-copy gene for each sample genome. All genes were then aligned using the multiple sequence alignment program MAFFT version 7.475? (Katoh 2002) with the parameters --maxiterate 1000

--localpair --reorder. MAFFT alignments were concatenated with a custom script, which also provided a partition file for subsequent tree reconstruction. Concatenated sequences and partitions file were then used for phylogenetic through IQ-TREE version (Nguyen et al. 2015) using automatic model finder (Kalyaanamoorthy et al. 2017) and 1000 ultrafast bootstrap replicates optimized using the --bnni flag (Hoang et al. 2018).

Multi-gene summary coalescent tree analysis was conducted in the same manner as previously stated, except that each gene profile was aligned individually rather than concatenated. Each gene alignment was then used to construct a phylogenetic tree in the same manner listed previously. Coalescent analysis was performed using all 2,983 gene trees to construct a consensus tree using ASTRAL-III (Zhang et al. 2018). Both trees were congruent with one another, and the concatenated gene tree was chosen to be used as a constraint tree for further DNA barcode analysis.

Molecular dating and divergence of phylogenomic data

Molecular divergence dating analysis was conducted on our *Deconica*, *Psilocybe*, and outgroup taxa concatenated tree (Supplementary Figure 1) utilizing two different methods with a calibration range of 71 mya (Ruiz-Dueñas et al. 2021) to 57 mya (Varga et al. 2019), representative of the divergence of the family *Hymenogastraceae*. The first method utilized uncorrelated penalized likelihood with the “relaxed” model in the R package APE version 6.6–2 (Paradis and Schliep 2019). The second method utilized was through the GUI for pyr8s version (0_1_win) (Sanderson 2003) utilizing the min-max age range calibration of 57–71 mya, with all other parameters set to default. Methods using Bayesian analysis such as BEAST2 (Bouckaert et al. 2014) were not used as the computational time needed to active convergence on a dataset of

this size was unachievable. Trees and divergence times were visualized using FigTree version 1.4.4 (http://tree.bio.ed.ac.uk/software/figtree/).

ITS, EF1a, RPB1, and RPB2 gene extraction and phylogenetic analysis

DNA barcodes were extracted bioinformatically with an in-house pipeline. In brief, 10859 complete fungal ITS, 487 EF1a, 639 RPB1, and 937 RPB2 with conserved exon sequences from AFTOL (Lutzoni et al. 2004) were aligned respectively with MAFFTversion 7.475 (Katoh 2002) and used to generate an HMM profile with hmmr version 3.1b2 (hmmer.org). The HMM profile for fungal ITS was used with PathRacer (SPAdes-3.15.0-pathracer-2020-12-20-dev) (Shlemov and Korobeynikov 2019) in conjunction with the assembly graph output from SPAdes to produce a most probable sequence path for the HMM provided. ITS sequences were manually trimmed from edge sequence outputs. Sequences of EF1a, RPB1, and RPB2 were extracted from edge sequence outputs with Exonerate using the flag-protein2genome and a query of GenBank proteins sequences from *Psilocybe cyanescens* (ADI71893.1- EF1a, AHB18799.1-RPB1, and AHH34099.1-RPB2). All *Psilocybe* s.s. sequences corresponding to the same loci (ITS, EF1a, RPB1, RPB2) were retrieved from NCBI as well as all species hypotheses (SH) ITS sequences from the curated fungal database UNITE (Abarenkov et al. 2010). Each data set from NCBI was checked for overlap of different genes for a single vouchered specimen. Due to the robust nodal support of our phylogenomic species tree, analysis was performed using the concatenated gene tree constructed with only *Psilocybe* specimens in conjunction with all public datasets.

Phylogenetic trees for each barcode were constructed using IQ-TREE with the same parameters as above, except for using a constraint tree derived from the concatenated gene tree to preserve the well-supported topology from the phylogenomic analysis.

Microscopic characteristics to confirm misidentification

For microscopic investigation, hand sections were made from the pileus to observe basidiospores and cheilocystidia. Sections were mounted in 5% KOH after being rehydrated with 70% ethanol. At minimum of 25 measurements of each microstructure were taken using a 100 × oil-inmersion objective on Zeiss K-7 light microscopes and photographed using a Zeiss Axioscop 40 with Zen 2.3 lite.

Gene prediction of psilocybin gene cluster and construction of gene trees

With robust phylogenomic data, questions outside the realm of phylogenetic species relationships can now be explored, such as the evolution of specific traits and their ecological role. In particular, the psychoactive secondary metabolites, psilocybin and psilocin, first identified in *Psilocybe* mushrooms, are of particular interest due to their high therapeutic potential (Frood 2008; Lowe et al. 2021; Marks and Cohen 2021). We used gene prediction and an RBB bioinformatic extraction method to identify each gene from the clusters in our genomes and phylogenetic analysis of each of our genes was generally congruent with our species tree (Figure 2), except for the P_{450}-encoding PsiH.

Due to the diploid nature of our genomes, we first used the software package Redundans version 0.14a (Pryszcz and Gabaldón 2016) to phase our assemblies before gene prediction. Psilocybin gene cluster detection was performed using the Augustus version 3.4.0 gene prediction software (Stanke et al. 2006) with the flags –singlestrand=true to predict genes independently on each strand, and using the coprinus_cinereus training set. Following gene

prediction, the most likely psilocybin BGC for each species was chosen as follows: using the protein sequences for PsiD, PsiK, PsiH, and PsiM based on the publicly available chromosomal level assembly for *P. cubensis* (McKernan et al. 2021), we used BLASTP with default parameters to search for homologs in the predicted translated proteins for each species. The top three hits for each gene were then used together to find putative clusters by examining the gene numbers assigned by Augustus. Putative "clusters" were identified as any subset of the 21 genes where the predicted gene numbers of any gene within the subset was at most two genes away from one other gene in the subset. This set of computationally-generated putative psilocybin clusters was then manually curated by querying the top three hits against the Psi gene sequences from the chromosomal assembly of *P. cubensis* using BLASTn to measure their similarities. The largest subset with high similarities to the Psi genes was chosen as the cluster candidate for each *Psilocybe* species (Figure 2). To corroborate our gene predictions, we utilized Exonerate with the same Psi protein queries. Phylogenetic trees were generated as above, without utilizing the species constraint tree, then visualized and midpoint-rooted using FigTree 1.4.4.

PsiD molecular analysis with *Psilocybe* and non-*Psilocybe* psilocybin producers

PsiD nucleotide sequences extracted through exonerate were transcribed utilizing codon-aware multiple sequence alignment through HYPHY version 2.5.36 (Pond et al. 2005) following the tutorial outlined at: https://github.com/veg/hyphy-analyses/blob/master/codon-msa/README.md

Extracted PsiD amino acid sequences were combined with the PsiD ammino acid sequences published in Reynolds et al. (2018), undergoing multiple sequence alignment and phylogenetic analysis under the same parameters used for individual gene trees.

Psilocybin producing taxa phylogenetic analysis and divergence dating

In order to assess the relative timing of psilocybin biosynthesis across the mushrooms, a dataset was constructed of all publicly available sequences of the ribosomal large subunit DNA region (28S; downloaded from NCBI on 14 August 2022) for *Conocybe/Pholiotina,Gymnopilus, Panaeolus, Pluteus, and Psilocybe.*. A sequence of *Calocybe gambosa* (Fr.) Donk was used as an outgroup. Due to the poor overlap between taxa for different gene regions, the 28S region had the best species representation that could be aligned across all genera. Multiple sequence alignment was performed using the L-INS-i algorithm in MAFFT. Phylogenetic analysis was performed under maximum likelihood using IQ-Tree with automatic model selection and up to 1000 nonparametric rapid bootstraps. Branch lengths were converted to relative time using uncorrelated penalized likelihood implemented in the 'chronos' function in the R package 'ape'. Dates were inferred from the distance of the nodes from the tips based on the distance to the stem node for *Psilocybe* estimated, above. Additionally, pyr8s was run with a time constraint of 136 mya, corresponding to the divergence date of *Agaricales* (He et al. 2019), as well as in scalar mode for comparison (Supplementary Table 3).

Citations:

Abarenkov K., Henrik Nilsson R., Larsson K., Alexander I.J., Eberhardt U., Erland S., Høiland K., Kjøller R., Larsson E., Pennanen T., Sen R., Taylor A.F.S., Tedersoo L., Ursing B.M., Vrålstad T., Liimatainen K., Peintner U., Kõljalg U. 2010. The UNITE database for molecular identification of fungi – recent updates and future perspectives. New Phytologist. 186:281–285.

Adams A.M., Kaplan N.A., Wei Z., Brinton J.D., Monnier C.S., Enacopol A.L., Ramelot T.A., Jones J.A. 2019. In vivo production of psilocybin in *E. coli*. Metabolic Engineering. 56:111–119.
Adams G.C., Kropp B.R. 1996. Athelia arachnoidea , the sexual state of Rhizoctonia carotae , a pathogen of carrot in cold storage. Mycologia. 88:459–472.

Aime M.C., Miller A.N., Aoki T., Bensch K., Cai L., Crous P.W., Hawksworth D.L., Hyde K.D., Kirk P.M., Lücking R., May T.W., Malosso E., Redhead S.A., Rossman A.Y., Stadler M., Thines M., Yurkov A.M., Zhang N., Schoch C.L. 2021. How to publish a new fungal species, or name, version 3.0. IMA Fungus. 12:11.

Alban-J. G., Terán M. del C., Robles-U. M., Quinde F., Niveiro N. 2021. *Psilocybe cubensis* (Agaricales, Basidiomycota) en Ecuador. Lilloa. 58:86–94.

Andrew C., Diez J., James T.Y., Kauserud H. 2019. Fungarium specimens: a largely untapped source in global change biology and beyond. Phil. Trans. R. Soc. B. 374:20170392.

Araújo A.M., Carvalho F., Bastos M. de L., Guedes de Pinho P., Carvalho M. 2015. The hallucinogenic world of tryptamines: an updated review. Arch Toxicol. 89:1151–1173.

Arvidsson, L. 1976. Athelia arachnoidea (Berk.) Jill. and its influence on epiphytic cryptogams in urban areas. Giteborgs Svampklubbs Arsskr. 1975-1976

Arvidsson, L. 1978. Svampangrepp på lavar - en orsak till lavöken. Svensk Botanisk Tidskrift, 72: 285-292.

Awan A.R., Winter J.M., Turner D., Shaw W.M., Suz L.M., Bradshaw A.J., Ellis T., Dentinger B.T.M. 2018. Convergent evolution of psilocybin biosynthesis by psychedelic mushrooms. bioRxiv.:374199.

Bankevich A., Nurk S., Antipov D., Gurevich A.A., Dvorkin M., Kulikov A.S., Lesin V.M., Nikolenko S.I., Pham S., Prjibelski A.D., Pyshkin A.V., Sirotkin A.V., Vyahhi N., Tesler G., Alekseyev M.A., Pevzner P.A. 2012. SPAdes: A New Genome assembly algorithm and its applications to single-cell sequencing. Journal of Computational Biology. 19:455–477.

Borovička J., Noordeloos M.E., Gryndler M., Oborník M. 2011. Molecular phylogeny of *Psilocybe cyanescens* complex in Europe, with reference to the position of the secotioid *Weraroa novae-zelandiae*. Mycol Progress. 10:149–155.

726 Bouckaert R., Heled J., Kühnert D., Vaughan T., Wu C.-H., Xie D., Suchard M.A., Rambaut A.,
727 Drummond A.J. 2014. BEAST 2: A Software Platform for Bayesian Evolutionary Analysis.
728 PLoS Comput Biol. 10:e1003537.
729
730 Boyce G.R., Gluck-Thaler E., Slot J.C., Stajich J.E., Davis W.J., James T.Y., Cooley J.R.,
731 Panaccione D.G., Eilenberg J., De Fine Licht H.H., Macias A.M., Berger M.C., Wickert K.L.,
732 Stauder C.M., Spahr E.J., Maust M.D., Metheny A.M., Simon C., Kritsky G., Hodge K.T.,
733 Humber R.A., Gullion T., Short D.P.G., Kijimoto T., Mozgai D., Arguedas N., Kasson M.T.
734 2019. Psychoactive plant- and mushroom-associated alkaloids from two behavior modifying
735 cicada pathogens. Fungal Ecol. 41:147–164.
736
737 Bradshaw A.J., Backman T.A., Ramírez-Cruz V., Forrister D.L., Winter J.M., Guzmán-Dávalos
738 L., Furci G., Stamets P., Dentinger B.T.M. 2022. DNA Authentication and Chemical Analysis of
739 Psilocybe Mushrooms Reveal Widespread Misdeterminations in Fungaria and Inconsistencies in
740 Metabolites. Appl Environ Microbiol.:e01498-22.
741
742 Briggs J.C. 1991. A Cretaceous-Tertiary mass extinction? Were most of Earth's species killed
743 off? Bioscience. 41:619–624.
744
745 Caiafa M.V., Smith M.E. 2022. Polyphyly, asexual reproduction and dual trophic mode in
746 *Buchwaldoboletus*. Fungal Ecol.. 56:101141.
747
748 Chen S., Zhou Y., Chen Y., Gu J. 2018. fastp: an ultra-fast all-in-one FASTQ preprocessor.
749 Bioinformatics. 34:i884–i890.
750
751 Chethana K.W.T., Manawasinghe I.S., Hurdeal V.G., Bhunjun C.S., Appadoo M.A., Gentekaki
752 E., Raspé O., Promputtha I., Hyde K.D. 2021. What are fungal species and how to delineate
753 them? Fungal Divers. 109:1–25.
754
755 Christiansen A., Baum R., Witt P.N. 1962. Changes in spider webs brought about by mescaline,
756 psilocybin and an increase in body weight. Journal of Pharmacology and Experimental
757 Therapeutics. 136:31–37.
758
759 Christiansen A.L., Rasmussen K.E., Høiland K. 1984. Detection of psilocybin and psilocin in
760 Norwegian species of Pluteus and *Conocybe*. Planta Med. 50:341–343.
761
762 Cortés-Pérez A., Ramírez-Guillén F., Guzmán G., Guzmán-Dávalos L., Rockefeller A., Ramírez-
763 Cruz V. 2020. Type studies in five species of *Psilocybe* (Agaricales, Basidiomycota). Nova
764 Hedwigia. 112:197–221.
765

766 Dentinger B.T.M., Gaya E., O'Brien H., Suz L.M., Lachlan R., Díaz-Valderrama J.R., Koch
767 R.A., Aime M.C. 2016. Tales from the crypt: genome mining from fungarium specimens
768 improves resolution of the mushroom tree of life. Biol. J. Linn. Soc. 117:11–32.
769 Dörner S., Rogge K., Fricke J., Schäfer T., Wurlitzer J.M., Gressler M., Pham D.N.K., Manke
770 D.R., Chadeayne A.R., Hoffmeister D. 2022. Genetic survey of *Psilocybe* natural products.
771 ChemBioChem.:cbic.202200249.
772
773 Ewels P., Magnusson M., Lundin S., Käller M. 2016. MultiQC: summarize analysis results for
774 multiple tools and samples in a single report. Bioinformatics. 32:3047–3048.
775
776 French A.S., Simcock K.L., Rolke D., Gartside S.E., Blenau W., Wright G.A. 2014. The role of
777 serotonin in feeding and gut contractions in the honeybee. J Insect Physiol. 61:8–15.
778
779 Fricke J., Blei F., Hoffmeister D. 2017. Enzymatic synthesis of psilocybin. Angew. Chem. Int.
780 Ed. 56:12352–12355.
781
782 Froese T., Guzmán G., Guzmán-Dávalos L. 2016. On the origin of the genus *Psilocybe* and its
783 potential ritual use in ancient Africa and Europe. Econ Bot. 70:103–114.
784
785 Frood A. 2008. Benefits of "magic mushroom" therapy long lasting. Nature.:news.2008.934.
786 Gartz J. 1987. Occurrence of psilocybin and baeocystin in fruit bodies of *Pluteus salicinus*.
787 Planta Med. 53:290–291.
788
789 Grant A.J., Dickens J.C. 2011. Functional characterization of the octenol receptor neuron on the
790 maxillary palps of the yellow fever mosquito, *Aedes aegypti*. PLoS ONE. 6:e21785.
791
792 Grigoriev I.V., Nikitin R., Haridas S., Kuo A., Ohm R., Otillar R., Riley R., Salamov A., Zhao
793 X., Korzeniewski F., Smirnova T., Nordberg H., Dubchak I., Shabalov I. 2014. MycoCosm
794 portal: gearing up for 1000 fungal genomes. Nucl. Acids Res. 42:D699–D704.
795
796 Grigoriev I.V., Nordberg H., Shabalov I., Aerts A., Cantor M., Goodstein D., Kuo A.,
797 Minovitsky S., Nikitin R., Ohm R.A., Otillar R., Poliakov A., Ratnere I., Riley R., Smirnova T.,
798 Rokhsar D., Dubchak I. 2012. The genome portal of the Department of Energy Joint Genome
799 Institute. Nucleic Acids Research. 40:D26–D32.
800
801 Guy St.C. Slater. 2000. exonerate: A generic sequence comparison tool
802 (http://www.ebi.ac.uk/~guy/exonerate/)
803

Guzmán G. 1983. The genus *Psilocybe*: a systematic revision of the known species including the history, distribution, and chemistry of the hallucinogenic species. Vaduz [Liechtenstein]: J. Cramer.

Guzmán G. 1995. Supplement to the monograph of genus *Psilocybe*. In: Taxonomic monographs of Agaricales. Edite by O. Petrini and E. Horak. Bibl. Myco. 159:91–141.

Guzman G. 2005. Species diversity of the genus *Psilocybe* (Basidiomycotina, Agaricales, Strophariaceae) in the world mycobiota, with special attention to hallucinogenic properties. Int J Med Mushr. 7:305–332.

Guzmán G., Allen J., Gartz J. 1998. A worldwide geographical distribution of the neurotropic fungi, an analysis and discussion. Ann Mus Civ Rovereto. 14;189-280

Guzmán G., Vergeer P.P. 1978. Index of taxa in the genus *Psilocybe*. Mycotaxon. 6:464–476.

Hall D.R., Beevor P.S., Cork A., Nesbitt B.F., Vale G.A. 1984. 1-Octen-3-ol. A potent olfactory stimulant and attractant for tsetse isolated from cattle odours. Int. J. Trop. Insect Sci. 5:335–339.

He M.-Q., Zhao R.-L., Hyde K.D., Begerow D., Kemler M., Yurkov A., McKenzie E.H.C., Raspé O., Kakishima M., Sánchez-Ramírez S., Vellinga E.C., Halling R., Papp V., Zmitrovich I.V., Buyck B., Ertz D., Wijayawardene N.N., Cui B.-K., Schoutteten N., Liu X.-Z., Li T.-H., Yao Y.-J., Zhu X.-Y., Liu A.-Q., Li G.-J., Zhang M.-Z., Ling Z.-L., Cao B., Antonín V., Boekhout T., da Silva B.D.B., De Crop E., Decock C., Dima B., Dutta A.K., Fell J.W., Geml J., Ghobad-Nejhad M., Giachini A.J., Gibertoni T.B., Gorjón S.P., Haelewaters D., He S.-H., Hodkinson B.P., Horak E., Hoshino T., Justo A., Lim Y.W., Menolli N., Mešić A., Moncalvo J.-M., Mueller G.M., Nagy L.G., Nilsson R.H., Noordeloos M., Nuytinck J., Orihara T., Ratchadawan C., Rajchenberg M., Silva-Filho A.G.S., Sulzbacher M.A., Tkalčec Z., Valenzuela R., Verbeken A., Vizzini A., Wartchow F., Wei T.-Z., Weiß M., Zhao C.-L., Kirk P.M. 2019. Notes, outline and divergence times of Basidiomycota. Fungal Diversity. 99:105–367.

Hoang D.T., Chernomor O., von Haeseler A., Minh B.Q., Vinh L.S. 2018. UFBoot2: Improving the Ultrafast Bootstrap Approximation. Molecular Biology and Evolution. 35:518–522.

Hoffmeister D., Keller N.P. 2007. Natural products of filamentous fungi: enzymes, genes, and their regulation. Nat. Prod. Rep. 24:393–416.

Hofmann A., Heim R., Brack A., Kobel H., Frey A., Ott H., Petrzilka Th., Troxler F. 1959. Psilocybin und psilocin, zwei psychotrope Wirkstoffe aus mexikanischen Rauschpilzen. Helv. Chim. Acta. 42:1557–1572.

Joulain D. 1993. The scent of orchids. Olfactory and chemical investigations by Roman Kaiser. Co-published by Givaudan-Roure, Dübendorf, Switzerland, and Elsevier, Amsterdam, 1993. ISBN 0–444–89841–7. Flavour Fragr. J. 8:295–295.

Kaim A. 2002. Gradual evolution of the Early Cretaceous marine gastropod *Rissoina* lineage in central Poland. Acta Palaeontologica Polonica. 47(4): 667–672.Kaiser R. 2006. Flowers and fungi use scents to mimic each other. Science. 311:806–807.

Kalyaanamoorthy S., Minh B.Q., Wong T.K.F., von Haeseler A., Jermiin L.S. 2017. ModelFinder: fast model selection for accurate phylogenetic estimates. Nat Methods. 14:587–589.

Katoh K. 2002. MAFFT: a novel method for rapid multiple sequence alignment based on fast Fourier transform. Nucleic Acids Research. 30:3059–3066.

Kirk, P.M., Cannon, P.F., Minter, D.W. & Stalpers, J.A. 2008. Ainsworth & Bisby's Dictionary of the Fungi. 10th Edition. CABI Europe.

Kline D.L., Hagan D.V., Wood J.R. 1994. Culicoides responses to 1-octen-3-ol and carbon dioxide in salt marshes near Sea Island, Georgia, U.S.A. Med Vet Entomol. 8:25–30.

Konkel Z., Scott K., Slot J.C. 2021. Draft Genome Sequence of the Termite-Associated “Cuckoo Fungus,” *Athelia* (Fibularhizoctonia) sp. TMB Strain TB5. Microbiol Resour Announc. 10: e01230-20.

Lenz C., Sherwood A., Kargbo R., Hoffmeister D. 2021. Taking different roads: l □tryptophan as the origin of *Psilocybe* natural products. ChemPlusChem. 86:28–35.

Lenz C., Wick J., Braga D., García□Altares M., Lackner G., Hertweck C., Gressler M., Hoffmeister D. 2020. Injury□triggered blueing reactions of *Psilocybe* “magic” mushrooms. Angew. Chem. Int. Ed. 59:1450–1454.

Liimatainen K., Kim J.T., Pokorny L., Kirk P.M., Dentinger B., Niskanen T. 2022. Taming the beast: a revised classification of Cortinariaceae based on genomic data. Fungal Diversity. 112:89–170.

Lowe H., Toyang N., Steele B., Valentine H., Grant J., Ali A., Ngwa W., Gordon L. 2021. The therapeutic potential of psilocybin. Molecules. 26:2948.

884 Lutzoni F., Kauff F., Cox C.J., McLaughlin D., Celio G., Dentinger B., Padamsee M., Hibbett
885 D., James T.Y., Baloch E., Grube M., Reeb V., Hofstetter V., Schoch C., Arnold A.E.,
886 Miadlikowska J., Spatafora J., Johnson D., Hambleton S., Crockett M., Shoemaker R., Sung G.,
887 Lücking R., Lumbsch T., O'Donnell K., Binder M., Diederich P., Ertz D., Gueidan C., Hansen
888 K., Harris R.C., Hosaka K., Lim Y., Matheny B., Nishida H., Pfister D., Rogers J., Rossman A.,
889 Schmitt I., Sipman H., Stone J., Sugiyama J., Yahr R., Vilgalys R. 2004. Assembling the fungal
890 tree of life: progress, classification, and evolution of subcellular traits. Am. J. Bot. 91:1446–
891 1480.
892
893 Ma T., Feng Y., Lin X.-F., Karunarathna S.C., Ding W.-F., Hyde K.D. 2014. *Psilocybe*
894 *chuxiongensis,* a new bluing species from subtropical China. Phytotaxa. 156:211.
895 Marks M., Cohen I.G. 2021. Psychedelic therapy: a roadmap for wider acceptance and
896 utilization. Nat Med.
897
898 Matheny P.B., Curtis J.M., Hofstetter V., Aime M.C., Moncalvo J.-M., Ge Z.-W., Yang Z.-L.,
899 Slot J.C., Ammirati J.F., Baroni T.J., Bougher N.L., Hughes K.W., Lodge D.J., Kerrigan R.W.,
900 Seidl M.T., Aanen D.K., DeNitis M., Daniele G.M., Desjardin D.E., Kropp B.R., Norvell L.L.,
901 Parker A., Vellinga E.C., Vilgalys R., Hibbett D.S. 2006. Major clades of Agaricales: a
902 multilocus phylogenetic overview. Mycologia. 98:982–995.
903
904 Matsuura K. 2005. Distribution of termite egg-mimicking fungi ("termite balls") in
905 Reticulitermes spp. (Isoptera: Rhinotermitidae) nests in Japan and the United States. Appl.
906 Entomol. Zool. 40:53–61.
907
908 McKernan K., Kane L.T., Crawford S., Chin C.-S., Trippe A., McLaughlin S. 2021. A draft
909 reference assembly of the *Psilocybe cubensis* genome. F1000Res. 10:281.
910
911 Milne N., Thomsen P., Mølgaard Knudsen N., Rubaszka P., Kristensen M., Borodina I. 2020.
912 Metabolic engineering of Saccharomyces cerevisiae for the de novo production of psilocybin and
913 related tryptamine derivatives. Metabolic Engineering. 60:25–36.
914
915 Moncalvo J.-M., Lutzoni F.M., Rehner S.A., Johnson J., Vilgalys R. 2000. Phylogenetic
916 relationships of agaric fungi based on nuclear large subunit ribosomal DNA sequences.
917 Systematic Biology. 49:278–305.
918
919 Moncalvo J.-M., Vilgalys R., Redhead S.A., Johnson J.E., James T.Y., Catherine Aime M.,
920 Hofstetter V., Verduin S.J.W., Larsson E., Baroni T.J., Greg Thorn R., Jacobsson S., Clémençon
921 H., Miller O.K. 2002. One hundred and seventeen clades of euagarics. Molecular Phylogenetics
922 and Evolution. 23:357–400.
923

924 Morris N., Taylor J. 2000. Global events and biotic interaction as controls on the evolution of
925 gastropods. In: Culver S.J., Rawson P.F., editors. Biotic Response to Global Change. Cambridge
926 University Press. p. 149–163.
927
928 Mycorrhizal Genomics Initiative Consortium, Kohler A., Kuo A., Nagy L.G., Morin E., Barry
929 K.W., Buscot F., Canbäck B., Choi C., Cichocki N., Clum A., Colpaert J., Copeland A., Costa
930 M.D., Doré J., Floudas D., Gay G., Girlanda M., Henrissat B., Herrmann S., Hess J., Högberg
931 N., Johansson T., Khouja H.-R., LaButti K., Lahrmann U., Levasseur A., Lindquist E.A., Lipzen
932 A., Marmeisse R., Martino E., Murat C., Ngan C.Y., Nehls U., Plett J.M., Pringle A., Ohm R.A.,
933 Perotto S., Peter M., Riley R., Rineau F., Ruytinx J., Salamov A., Shah F., Sun H., Tarkka M.,
934 Tritt A., Veneault-Fourrey C., Zuccaro A., Tunlid A., Grigoriev I.V., Hibbett D.S., Martin F.
935 2015. Convergent losses of decay mechanisms and rapid turnover of symbiosis genes in
936 mycorrhizal mutualists. Nat Genet. 47:410–415.
937
938 Neubauer T.A., Harzhauser M. 2022. Onset of Late Cretaceous diversification in Europe's
939 freshwater gastropod fauna links to global climatic and biotic events. Sci Rep. 12:2684.
940 Nguyen L.-T., Schmidt H.A., von Haeseler A., Minh B.Q. 2015. IQ-TREE: A fast and effective
941 stochastic algorithm for estimating maximum-likelihood phylogenies. Molecular Biology and
942 Evolution. 32:268–274.
943
944 Nichols C.D., Ronesi J., Pratt W., Sanders-Bush E. 2002. Hallucinogens and *Drosophila*: linking
945 serotonin receptor activation to behavior. Neuroscience. 115:979–984.
946
947 Noordeloos M.E. 2011. Strophariaceae s. l. Fungi Europaei 13. Edizioni Candusso,
948 Alassio, Italy.
949
950 Paradis E., Schliep K. 2019. ape 5.0: an environment for modern phylogenetics and evolutionary
951 analyses in R. Bioinformatics. 35:526–528.
952
953 Parks S.L., Goldman N. 2014. Maximum likelihood inference of small trees in the presence of
954 long branches. Systematic Biology. 63:798–811.
955
956 Passie T., Seifert J., Schneider U., Emrich H.M. 2002. The pharmacology of psilocybin.
957 Addiction Biology. 7:357–364.
958
959 Policha T., Davis A., Barnadas M., Dentinger B.T.M., Raguso R.A., Roy B.A. 2016.
960 Disentangling visual and olfactory signals in mushroom□mimicking Dracula orchids using
961 realistic three□dimensional printed flowers. New Phytol. 210:1058–1071.
962
963 Pond S.L.K., Frost S.D.W., Muse S.V. 2005. HyPhy: hypothesis testing using phylogenies.
964 Bioinformatics. 21:676–679.

Pryszcz L.P., Gabaldón T. 2016. Redundans: an assembly pipeline for highly heterozygous genomes. Nucleic Acids Res. 44:e113–e113.

Ramírez-Cruz V., Guzmán G., Villalobos-Arámbula A.R., Rodríguez A., Matheny P.B., Sánchez-García M., Guzmán-Dávalos L. 2013a. Phylogenetic inference and trait evolution of the psychedelic mushroom genus *Psilocybe* sensu lato (Agaricales). Botany. 91:573–591.

Ramírez-Cruz V., Guzmán G., Guzmán-Dávalos L. 2013b. Type studies of *Psilocybe* sensu lato (Strophariaceae, Agaricales). Sydowia Sydowia. 65 (*2): 277–319*.

Raup D.M., Boyajian G.E. 1988. Patterns of generic extinction in the fossil record. Paleobiology. 14:109–125.

Reynolds H.T., Vijayakumar V., Gluck-Thaler E., Korotkin H.B., Matheny P.B., Slot J.C. 2018. Horizontal gene cluster transfer increased hallucinogenic mushroom diversity. Evolution Letters. 2:88–101.

Riley R., Salamov A.A., Brown D.W., Nagy L.G., Floudas D., Held B.W., Levasseur A., Lombard V., Morin E., Otillar R., Lindquist E.A., Sun H., LaButti K.M., Schmutz J., Jabbour D., Luo H., Baker S.E., Pisabarro A.G., Walton J.D., Blanchette R.A., Henrissat B., Martin F., Cullen D., Hibbett D.S., Grigoriev I.V. 2014. Extensive sampling of basidiomycete genomes demonstrates inadequacy of the white-rot/brown-rot paradigm for wood decay fungi. Proc Natl Acad Sci USA. 111:9923–9928.

Ruiz-Dueñas F.J., Barrasa J.M., Sánchez-García M., Camarero S., Miyauchi S., Serrano A., Linde D., Babiker R., Drula E., Ayuso-Fernández I., Pacheco R., Padilla G., Ferreira P., Barriuso J., Kellner H., Castanera R., Alfaro M., Ramírez L., Pisabarro A.G., Riley R., Kuo A., Andreopoulos W., LaButti K., Pangilinan J., Tritt A., Lipzen A., He G., Yan M., Ng V., Grigoriev I.V., Cullen D., Martin F., Rosso M.-N., Henrissat B., Hibbett D., Martínez A.T. 2021. Genomic analysis enlightens Agaricales lifestyle evolution and increasing peroxidase diversity. Molecular Biology and Evolution. 38:1428–1446.

Sanderson M.J. 2003. R8s: inferring absolute rates of molecular evolution and divergence times in the absence of a molecular clock. Bioinformatics. 19:301–302.

Schoch C.L., Seifert K.A., Huhndorf S., Robert V., Spouge J.L., Levesque C.A., Chen W., Fungal Barcoding Consortium, Fungal Barcoding Consortium Author List, Bolchacova E., Voigt K., Crous P.W., Miller A.N., Wingfield M.J., Aime M.C., An K.-D., Bai F.-Y., Barreto R.W., Begerow D., Bergeron M.-J., Blackwell M., Boekhout T., Bogale M., Boonyuen N., Burgaz

A.R., Buyck B., Cai L., Cai Q., Cardinali G., Chaverri P., Coppins B.J., Crespo A., Cubas P., Cummings C., Damm U., de Beer Z.W., de Hoog G.S., Del-Prado R., Dentinger B., Dieguez-Uribeondo J., Divakar P.K., Douglas B., Duenas M., Duong T.A., Eberhardt U., Edwards J.E., Elshahed M.S., Fliegerova K., Furtado M., Garcia M.A., Ge Z.-W., Griffith G.W., Griffiths K., Groenewald J.Z., Groenewald M., Grube M., Gryzenhout M., Guo L.-D., Hagen F., Hambleton S., Hamelin R.C., Hansen K., Harrold P., Heller G., Herrera C., Hirayama K., Hirooka Y., Ho H.-M., Hoffmann K., Hofstetter V., Hognabba F., Hollingsworth P.M., Hong S.-B., Hosaka K., Houbraken J., Hughes K., Huhtinen S., Hyde K.D., James T., Johnson E.M., Johnson J.E., Johnston P.R., Jones E.B.G., Kelly L.J., Kirk P.M., Knapp D.G., Koljalg U., Kovacs G.M., Kurtzman C.P., Landvik S., Leavitt S.D., Liggenstoffer A.S., Liimatainen K., Lombard L., Luangsa-ard J.J., Lumbsch H.T., Maganti H., Maharachchikumbura S.S.N., Martin M.P., May T.W., McTaggart A.R., Methven A.S., Meyer W., Moncalvo J.-M., Mongkolsamrit S., Nagy L.G., Nilsson R.H., Niskanen T., Nyilasi I., Okada G., Okane I., Olariaga I., Otte J., Papp T., Park D., Petkovits T., Pino-Bodas R., Quaedvlieg W., Raja H.A., Redecker D., Rintoul T.L., Ruibal C., Sarmiento-Ramirez J.M., Schmitt I., Schussler A., Shearer C., Sotome K., Stefani F.O.P., Stenroos S., Stielow B., Stockinger H., Suetrong S., Suh S.-O., Sung G.-H., Suzuki M., Tanaka K., Tedersoo L., Telleria M.T., Tretter E., Untereiner W.A., Urbina H., Vagvolgyi C., Vialle A., Vu T.D., Walther G., Wang Q.-M., Wang Y., Weir B.S., Weiss M., White M.M., Xu J., Yahr R., Yang Z.L., yurkov A., Zamora J.-C., Zhang N., Zhuang W.-Y., Schindel D. 2012. Nuclear ribosomal internal transcribed spacer (ITS) region as a universal DNA barcode marker for Fungi. Proceedings of the National Academy of Sciences. 109:6241–6246.

Wasson RG. 1957. Seeking the magic mushroom. *Life* 49(19):100–102, 109–120.

Shlemov A., Korobeynikov A. 2019. PathRacer: racing Profile HMM Paths on Assembly Graph. In: Holmes I., Martín-Vide C., Vega-Rodríguez M.A., editors. Algorithms for Computational Biology. Cham: Springer International Publishing. p. 80–94.

Singer R., Smith A.H. 1958. Mycological investigations on teonanacatl, the Mexican hallucinogenic mushroom. Part II. A Taxonomic Monograph of *Psilocybe*, Section Caerulescentes. Mycologia. 50:262.

Sohl N.F. 1987. Cretaceous gastropods: contrasts between Tethys and the temperatepProvinces. Journal of Paleontology. 61:1085–1111.

Takken W., Kline D.L. 1989. Carbon dioxide and 1-octen-3-ol as mosquito attractants. J Am Mosq Control Assoc. 5:311–316.

Tremble K., Suz L.M., Dentinger B.T.M. 2020. Lost in translation: Population genomics and long-read sequencing reveals relaxation of concerted evolution of the ribosomal DNA cistron. Molecular Phylogenetics and Evolution. 148:106804.

Varga T., Krizsán K., Földi C., Dima B., Sánchez-García M., Sánchez-Ramírez S., Szöllősi G.J., Szarkándi J.G., Papp V., Albert L., Andreopoulos W., Angelini C., Antonín V., Barry K.W., Bougher N.L., Buchanan P., Buyck B., Bense V., Catcheside P., Chovatia M., Cooper J., Dämon W., Desjardin D., Finy P., Geml J., Haridas S., Hughes K., Justo A., Karasiński D., Kautmanova I., Kiss B., Kocsubé S., Kotiranta H., LaButti K.M., Lechner B.E., Liimatainen K., Lipzen A., Lukács Z., Mihaltcheva S., Morgado L.N., Niskanen T., Noordeloos M.E., Ohm R.A., Ortiz-Santana B., Ovrebo C., Rácz N., Riley R., Savchenko A., Shiryaev A., Soop K., Spirin V., Szebenyi C., Tomšovský M., Tulloss R.E., Uehling J., Grigoriev I.V., Vágvölgyi C., Papp T., Martin F.M., Miettinen O., Hibbett D.S., Nagy L.G. 2019. Megaphylogeny resolves global patterns of mushroom evolution. Nat Ecol Evol. 3:668–678.

Wood W.F., Archer C.L., Largent D.L. 2001. 1-Octen-3-ol, a banana slug antifeedant from mushrooms. Biochemical Systematics and Ecology. 29:531–533.

Yin W., Keller N.P. 2011. Transcriptional regulatory elements in fungal secondary metabolism. J Microbiol. 49:329–339.

Zhang C., Rabiee M., Sayyari E., Mirarab S. 2018. ASTRAL-III: polynomial time species tree reconstruction from partially resolved gene trees. BMC Bioinformatics. 19:153.

Acknowledgments:

We acknowledge the Natural History Museum of Utah for its commitment to collaborative Science and the Genomics Core Facility, a part of the Health Sciences Cores at The University of Utah, for their input and high-quality work. Additionally, we acknowledge the numerous institutions that provided specimens for destructive sampling, many of which were rare and irreplaceable. Further, we wish to recognize the dedicated and hard work performed by Isabelle Galland and Talia A. Backman in their help processing many of these samples for DNA sequencing. Further, the authors wish to thank David Scott Flocken for his insight and thought-provoking conversations on the work generated here. Additionally, we would like to thank Jan Borovička and Oscar Castro-Jauregui for providing high-quality images and graciously allowing us to use them for publication. Additionally, we would like to thank Dr. Jason Slot for providing data from previous publications as well as intriguing conversions about Psilocybin evolution. VRC and LGD would like to thank the University of Guadalajara and CONACYT for their support of their research.

Data Availability:

Raw short-read sequences for this project have been deposited in the Sequence Read Archive (SRA) and assigned the bioproject number PRJNA904752 . Raw tree files, assemblies, gene prediction files, multiple sequence alignments, and *Psilocybe* constraint tree are available through Dryad under https://doi.org/10.5061/dryad.tmpg4f52s. Any code or specific script requests should be sent to the corresponding author.

Author contributions:

Alexander J Bradshaw performed all molecular processing of specimens, genome assembly, phylogenomic analysis, data analysis, and initial gene prediction in addition to preparing and writing this manuscript. Virginia Ramírez-Cruz contributed with outreach to collection institutions, microscopic confirmation of misidentified specimens, taxonomic confirmation and updating information as well as providing crucial insight into the preparation and editing of this manuscript. Ali R. Awan performed bioinformatic analysis to identify and extract the psilocybin gene cluster genes from each specimen for use in phylogenetic analysis and the preparation and writing of this manuscript. Giuliana Furci contributed with outreach to collection institutions and comments and additions to the manuscript. Laura Guzmán-Dávalos contributed with outreach to collection institutions and comments, additions, and editing of the manuscript. Paul Stamets contributed comments and additions to the manuscript, as well as high-resolution images for specimens. Bryn T.M. Dentinger provided funding, experimental, and data analysis guidance and assisted in preparing and editing this manuscript.

Competing interests:

Paul Stamets is the current CEO of Fungi Perfecti LLC , a co-founder of MycoMedica Life Sciences, PBC and has been awarded a U.S. patent, and has pending patents on the use of psilocybin mushrooms for improving mental health. All other authors report no conflicting interests in the body or intent of this work.

1110

Figures:

Figure 1: Pictorial representation of *Psilocybe* species

A, *Psilocybe azurescens* (image credit, Paul Stamets), **B**, *Psilocybe cyanescens* (image credit Bryn T.M. Dentinger), **C**, *Psilocybe semilanceat*a (image credit Paul Stamets), **D**, *Psilocybe zapotecorum* (image credit Bryn T.M. Dentinger), **E,** *Psilocybe cubensis* (image credit Oscar Castro-Jauregui) , **F**, *Psilocybe bohemica* (image credit Jan Borovička), **G**, *Psilocybe yungensis* (image credit Virginia Ramírez-Cruz), **H**, *Psilocybe mexicana* (image credit Oscar Castro-Jauregui).

Figure 2

***Psilocybe* species tree, psilocybin producing gene cluster order, and Individual phylogenetic trees of the four core psilocybin producing cluster genes**

Left: Maximum likelihood tree constructed from 2983 concatenated genes for *Psilocybe* vouchers with major groupings of *Psilocybe* labeled and type specimens in Red. Here we expand the known major groups, while also showing that group "C" is split, which is novel to this study. **Center:** Recovered psilocybin-producing genes along with order and orientation within their respective sample. **Right:** Maximum-likelihood trees for each of the four core genes from the psilocybin producing gene cluster, PsiD, PsiK, PsiM, and PsiH. Asterisks denote vouchers determined to be misidentified.

Fig 3: PsiD and associated ecological niches compared to psilocybin producing phylogenic analysis

Left: PsiD tree with associated ecological niches for *Psilocybe* , *Conocybe*/*Pholiotina* , *Pluteus* , *Gymnopilus* , and *Panaeolus,* ecological niches are represented symbolically next to sample label. **Right:** LSU phylogenetic tree of known psilocybin producing taxa, blue coloring and axis numbering correspond to psilocybin acquisitions. Asterisks denote vouchers determined to be misidentified.

Tables:

Table 1:

Voucher table of Specimens

Specimen voucher table for each sequenced specimen, including holding institution, catalog number, post sequencing determination, and type status of the sample if applicable.

Supplementary Figures:

SF 1- Concatenated phylogenetic tree with *Deconica* genomes

SF 2- ASTRAL-III phylogenetic species tree with *Deconica* genomes

SF 3- ITS phylogenetic tree using *Psilocybe* species constraint tree

SF 4- EF1a phylogenetic tree using *Psilocybe* species constraint tree

SF 5- RPB1 phylogenetic tree using *Psilocybe* species constraint tree

SF 6- RPB2 tree using *Psilocybe* species constraint tree

Supplementary Tables:

ST-1-Genome assembly and BUSCO stats for each specimen

ST-2- RBB gene numbers, contigs, clustering results, and RBB method comparison to Exonerate

ST-3- Divergence time analysis methods and results

Figure 1:

Figure 2:

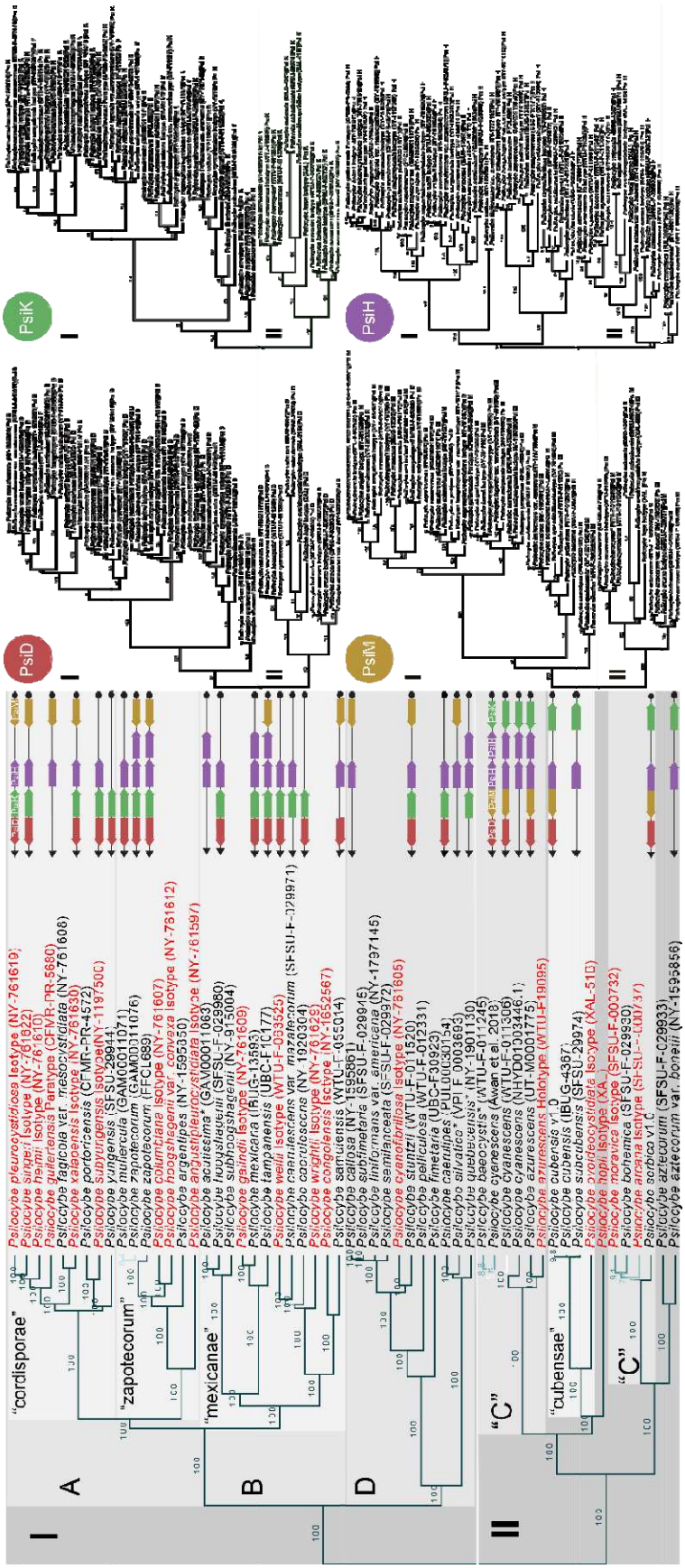

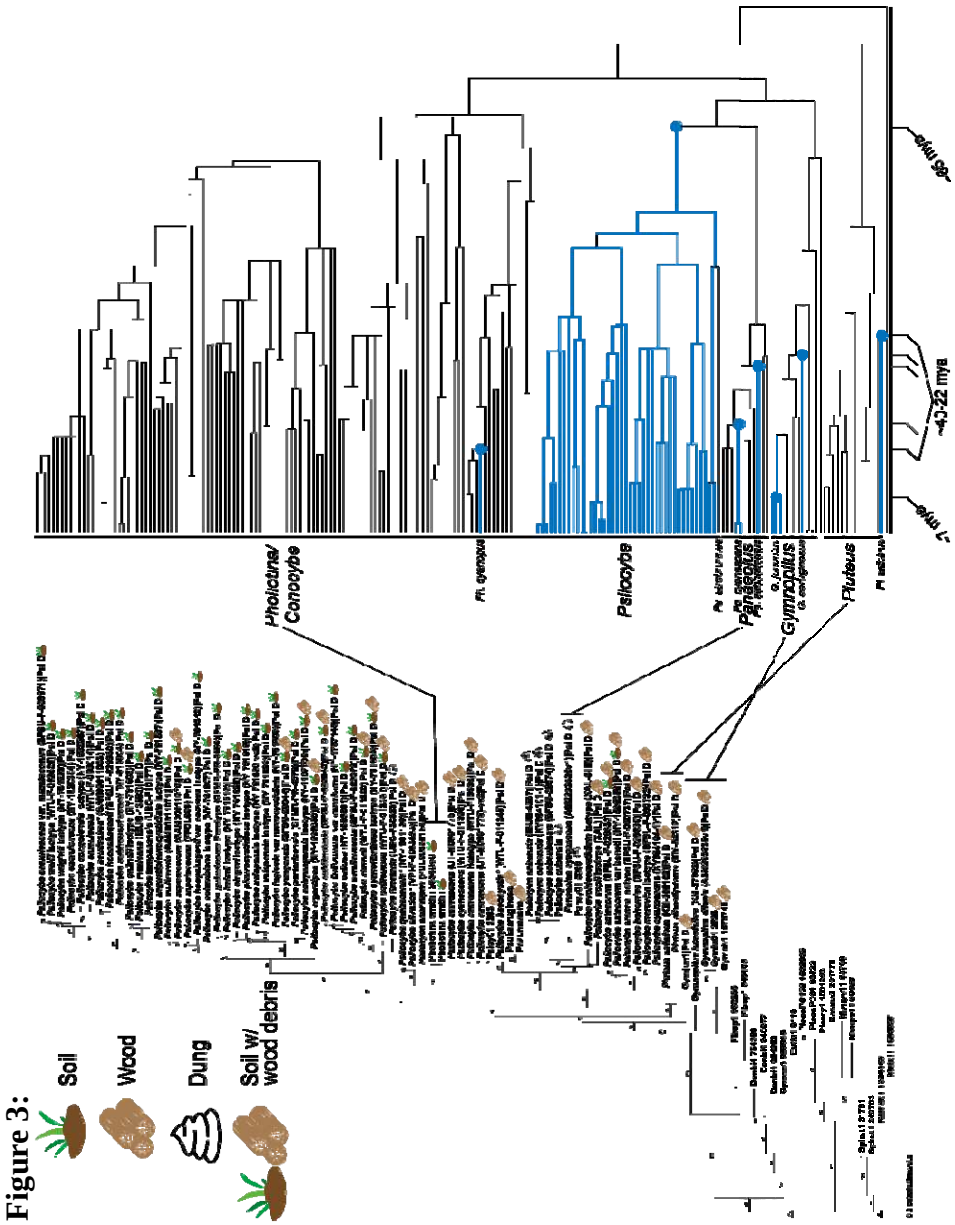

Figure 3:

Table 1:

Specimen	Voucher designation	Determination (current name in **bold**)	Locality	Type status	Collection year	Holding institution	Catalog number
Psilocybe_acutissima_GAM00011063	*Psilocybe acutissima*	***Psilocybe hoogshagenii* R. Heim**	Mexico	N/A	1967	GAM	GAM00011063
Psilocybe_angustipleurocystidiata_ISOTYPE_NY-761597	*Psilocybe angustipleurocystidiata*	***Psilocybe angustipleurocystidiata* Singer & A.H. Sm.**	Mexico	Isotype	1980	NY	761597
Psilocybe_arcana_ISOTYPE_SFSU-F-000737	*Psilocybe arcana*	***Psilocybe serbica* var. *arcana* (Borov. & Hlaváček) Borov., Oborník & Noordel.** =*Psilocybe arcana* Borov. & Hlaváček	Czech Republic	Isotype	2000	SFSU	SFSU-F-000737
Psilocybe_argentipes_NY-1595850	*Psilocybe argentipes*	***Psilocybe subcaerulipes* Hongo** = *Psilocybe argentipes* K. Yokoy.	Japan	N/A	1988	NY	1595850
Psilocybe_aztecorum_SFSU-F-029933	*Psilocybe aztecorum*	***Psilocybe aztecorum* R. Heim**	Mexico	N/A	1976	SFSU	SFSU-F-029933
Psilocybe_aztecorum_var._bonetii_NY-1595856	*Psilocybe aztecorum*	***Psilocybe aztecorum* R. Heim** = *Psilocybe aztecorum* var. *bonetii* (Guzmán) Guzmán	Mexico	N/A	1969	NY	1595856

Psilocybe_azurescens_WTU-F19095-HOLOTYPE	*Psilocybe azurescens*	***Psilocybe azurescens* Stamets & Gartz**	Oregon, USA	Holotype	1979	WTU	WTU-F-019095
Psilocybe_azurescens_UT-M0001775	*Psilocybe azurescens*	***Psilocybe azurescens* Stamets & Gartz**	Washington, USA	N/A	2020	NHMU	UT-M0001775
Psilocybe_baeocystis_WTU-F-011245	*Psilocybe baeocystis*	***Psilocybe cyanescens* Wakef.**	Washington, USA	N/A	1974	WTU	WTU-F-011245
Psilocybe_bohemica_SFSU-F-029930	*Psilocybe bohemica*	***Psilocybe serbica* var. *bohemica* (Šebek) Borov.**, Oborník & Noordel. = *Psilocybe bohemica* Šebek	Czech Republic	N/A	2004	SFSU	SFSU-F-029930
Psilocybe_caerulescens_NY-1920304	*Psilocybe caerulescens*	***Psilocybe caerulescens* Murrill**	Venezuela	N/A	1972	NY	1920304
Psilocybe_caerulescens_var._mazatecorum_SFSU-F-029971	*Psilocybe caerulescens*	***Psilocybe caerulescens* Murrill** = *Psilocybe caerulescens* var. *mazatecorum* R. Heim	Mexico	N/A	1967	SFSU	SFSU-F-029971
Psilocybe_caerulipes_PUL00030154	*Psilocybe caerulipes*	***Psilocybe caerulipes* (Peck) Sacc.**	Virginia, USA	N/A	1999	PUL	PUL00030154
Psilocybe_callosa_NY-1595861	*Psilocybe callosa*	***Psilocybe callosa* (Fr.) Gillet**	Oregon, USA	N/A	1976	NY	1595861
Psilocybe_columbiana_ISOTYPE_NY-761607	*Psilocybe columbiana*	***Psilocybe columbiana* Guzmán**	Columbia	Isotype	1971	NY	761607

Psilocybe_congolensis_ISOTYPE_NY-1652567	*Psilocybe congolensis*	***Psilocybe congolensis* Guzmán, S.C. Nixon & Cortés-Pérez**	Congo, Democratic Republic of the	Isotype	2011	NY	1652567
Psilocybe_cubensis_IBUG-4367	*Psilocybe cubensis*	***Psilocybe cubensis* (Earle) Singer**	Mexico	N/A	1993	IBUG	4367
Psilocybe_cyanescens_ALI	*Psilocybe cyanescens*	***Psilocybe cyanescens* Wakef.**	London	N/A	2014	KM	189047 & 234895
Psilocybe_cyanescens_WTU-F-011306	*Psilocybe cyanescens*	***Psilocybe cyanescens* Wakef.**	Washington, USA	N/A	1973	WTU	WTU-F-011306
Psilocybe_cyanofibrillosa_ISOTYPE_NY-761605	*Psilocybe cyanofibrillosa*	***Psilocybe cyanofibrillosa* Guzmán & Stamets**	Washington, USA	Isotype	1979	NY	761605
Psilocybe_fagicola_var._mesocystidiata_NY-761608	*Psilocybe fagicola*	***Psilocybe fagicola* R. Heim & Cailleux**	Mexico	Isotype	1975	NY	761608
Psilocybe_fimetaria_UBC-F30923	*Psilocybe fimetaria*	***Psilocybe fimetaria* (P.D. Orton) Watling**	Canada	N/A	2012	UBC	F30923
Psilocybe_galindii_ISOTYPE_NY-761609	*Psilocybe galindii*	***Psilocybe mexicana* R. Heim** = *Psilocybe galindoi* Guzmán	Mexico	Isotype	1974	NY	761609
Psilocybe_guilartensis_PARATYPE_CFMR-PR-5680	*Psilocybe guilartensis*	***Psilocybe guilartensis* Guzmán, F. Tapia & Nieves-Riv.**	Puerto Rico	Paratype	1999	CFMR	PR-5680

Psilocybe_heimii_ISOTYPE_NY-761610	*Psilocybe heimii*	***Psilocybe heimii* Guzmán**	Mexico	Isotype	1957	NY	761610
Psilocybe_hoogshageni_SFSU-F-029980	*Psilocybe hoogshageni*	***Psilocybe hoogshageni* R. Heim**	Mexico	N/A	1958	SFSU	SFSU-F-029980
Psilocybe_hoogshagenii_var._convexa_ISOTYPE_NY-761612	*Psilocybe hoogshagenii* var. *convexa* Guzmán	Likely a synonym of *Psilocybe sempervivae* R. Heim	Mexico	Isotype	1960	NY	761612
Psilocybe_hopii_ISOTYPE_XAL-#	*Psilocybe hopii*	***Psilocybe hopii* Guzmán & J. Greene**	Arizona, USA	Isotype	2010	XAL	no recorded catalog number
Psilocybe_liniformans_var._americana_NY-1797145	*Psilocybe liniformans*	***Psilocybe liniformans* Guzmán & Bas**	Oregon, USA	N/A	1979	NY	1797145
Psilocybe_mexicana_IBUG-13593	*Psilocybe mexicana*	***Psilocybe mexicana* R. Heim**	Mexico	N/A	2000	IBUG	13593
Psilocybe_moravica_ISOTYPE_SFSU-F-000732	*Psilocybe moravica*	***Psilocybe serbica* var. *moravica* (Borov.) Borov., Oborník & Noordel.** = *Psilocybe moravica* Borov.	Czech Republic	Isotype	2004	SFSU	SFSU-F-000732
Psilocybe_muliercula_GAM00011071	*Psilocybe muliercula*	***Psilocybe muliercula* Singer & A.H. Sm.**	Mexico	N/A	1958	GAM	GAM00011071
Psilocybe_ovoideocystidiata_ISOTYPE_XAL-51B	*Psilocybe ovoideocystidiata*	***Psilocybe ovoideocystidiata* Guzmán & Gaines**	Pennsylvania, USA	Isotype	2005	XAL	51B

Psilocybe_pelliculosa_WTU-F-012331	*Psilocybe pelliculosa*	***Psilocybe pelliculosa* (A.H. Sm.) Singer & A.H. Sm.**	Washington, USA	N/A	1952	WTU	WTU-F-012331
Psilocybe_pleurocystidiosa_ISOTYPE_NY-761619	*Psilocybe pleurocystidiosa*	***Psilocybe pleurocystidiosa* Guzmán**	Mexico	Isotype	1977	NY	761619
Psilocybe_portoricensis_CFMR-PR-4572	*Psilocybe portoricensis*	***Psilocybe portoricensis* Guzmán, Nieves-Riv. & F. Tapia**	Puerto Rico	N/A	1997	CFMR	PR-4572
Psilocybe_quebecensis_NY-1901130	*Psilocybe quebecensis*	***Psilocybe caerulipes* (Peck) Sacc.**	Canada	N/A	1995	NY	1901130
Psilocybe_samuiensis_WTU-F-055014	*Psilocybe samuiensis*	***Psilocybe samuiensis* Guzmán, Bandala & J.W. Allen**	Thailand	N/A	2001	WTU	WTU-F-055014
Psilocybe_semilanceata_SFSU-F-029972	*Psilocybe semilanceata*	***Psilocybe semilanceata* (Fr.) P. Kumm.**	Scotland	N/A	1973	SFSU	SFSU-F-029972
Psilocybe_silvatica_VPI-F-0003693	*Psilocybe silvatica*	***Psilocybe caerulipes* (Peck) Sacc.**	West Virginia, USA	N/A	2016	VPI	VPI-F-0003693
Psilocybe_singeri_ISOTYPE_NY-761622	*Psilocybe singeri*	***Psilocybe singeri* Guzmán**	Mexico	Isotype	1976	NY	761622
Psilocybe_stuntzii_WTU-F-011520	*Psilocybe stuntzii*	***Psilocybe stuntzii* Guzmán & J. Ott**	Washington, USA	N/A	1980	WTU	WTU-F-011520

Psilocybe_subcubensis_SFSU-29974	*Psilocybe subcubensis*	***Psilocybe subcubensis* Guzmán**	California, USA	N/A	1975	SFSU	SFSU-F-029974
Psilocybe_subfimetaria_SFSU-F-029945	*Psilocybe subfimetaria*	***Psilocybe subfimetaria* Guzmán & A.H. Sm.**	Oregon, USA	N/A	1976	SFSU	SFSU-F-029945
Psilocybe_subhoogshagenii_NY-915004	*Psilocybe subhoogshagenii*	***Psilocybe subhoogshagenii* Guzmán, M. Torres & Ram.-Guill.**	Ecuador	N/A	1987	NY	915004
Psilocybe_subyungensis_ISOTYPE_NY-1197500	*Psilocybe subyungensis*	***Psilocybe subyungensis* Guzmán**	Venezuela	Isotype	1972	NY	1197500
Psilocybe_tampanensis_UBC-F10177	*Psilocybe tampanensis*	***Psilocybe tampanensis* Guzmán & S.H. Pollock**	Texas, USA	N/A	1978	UBC	F10177
Psilocybe_weilii_ISOTYPE_WTU-F-063525	*Psilocybe weilii*	***Psilocybe weilii* Guzmán, Stamets & F. Tapia**	Georgia, USA	Isotype	1995	WTU	WTU-F-063525
Psilocybe_wrightii_ISOTYPE_NY-761629	*Psilocybe wrightii*	***Psilocybe wrightii* Guzmán**	Argentina	Isotype	1971	NY	761629
Psilocybe_xalapensis_ISOTYPE_NY-761630	*Psilocybe xalapensis*	***Psilocybe xalapensis* Guzmán & A. López**	Mexico	Isotype	1979	NY	761630
Psilocybe_zapotecorum_GAM00011076	*Psilocybe zapotecorum*	***Psilocybe zapotecorum* R. Heim**	Mexico	N/A	1967	GAM	GAM00011076

Psilocybe_yungensis_SFSU-29944	*Psilocybe yungensis*	***Psilocybe yungensis* Singer & A.H. Sm.**	Mexico	N/A	1958	SFSU	SFSU-F-029944
Psilocybe_zapotecorum_FFCL689	*Psilocybe zapotecorum*	***Psilocybe zapotecorum* R. Heim**	Chile	N/A	2020	FFCL	FCL689
Psilocybe_apelliculosa_UBC-F17545	*Psilocybe apelliculosa*	Probably a synonym of *Deconica castanella* (Peck) Noordel., according to Noordeloos (2011)	British Columbia, Canada	N/A	1997	UBC	UBC-F17545
Psilocybe_argentina_SFSU-F-029894	*Psilocybe argentina*	***Deconica argentina* (Speg.) Singer**	California, USA	N/A	1985	SFSU	SFSU-F-029894
Psilocybe_chionophila_OSC-113991	*Psilocybe chionophila*	***Deconica chionophila* (Lamoure) Noordel.**	Oregon, USA	N/A	2001	OSC	OSC-113991
Psilocybe_clavata_ISOTYPE_NY-761604	*Psilocybe clavata* Guzmán	***Deconica clavata* (Guzmán) Bradshaw, Ram.-Cruz & Dentinger, comb. nov.**	Mexico	Isotype	1978	NY	NY-761604
Psilocybe_fuliginosa_NY-1901148	*Psilocybe fuliginosa*	***Deconica* sp.**	Montana, USA	N/A	1981	NY	NY-1901148
Psilocybe_laticystis_UBC-F16759	*Psilocybe laticystis*	***Kuehneromyces* sp.**	British Columbia, Canada	N/A	2008	UBC	UBC-F16759

Psilocybe_lazoi_ISOTYPE_NY-761614	*Psilocybe lazoi*	***Deconica lazoi* (Singer) Bradshaw, Ram.-Cruz & Dentinger, comb. nov.**	Colchagua Province, La Viñita, Pumanque	Isotype	1967	NY	NY-761614
Psilocybe_magica_OSC-111954	*Psilocybe magica*	***Deconica magica* (Svrček) Noordel.**	Washington, USA	N/A	2005	OSC	OSC-111954
Psilocybe_montana_OSC-113978	*Psilocybe montana*	***Deconica montana* (Pers.) P.D. Orton**	Oregon, USA	N/A	2001	OSC	OSC-113978
Psilocybe_phyllogena_OSC-114015	*Psilocybe phyllogena*	***Deconica phyllogena* (Sacc.) Noordel.**	Oregon, USA	N/A	2001	OSC	OSC-114015
Psilocybe_polytrichophila_NY-1901129	*Psilocybe polytrichophila*	***Deconica* sp.**	New Jersey, USA	N/A	1984	NY	NY-1901129
Psilocybe_rhomboidospora_CMMF003424	*Psilocybe rhomboidospora*	***Deconica rhomboidospora* G.F. Atk.**	Québec, Canada	N/A	2000	CMMF	CMMF003424
Psilocybe_sabulosa_UBC-F13505	*Psilocybe sabulosa*	***Strophariaceae***	British Columbia, Canada	N/A	1983	UBC	UBC-F13505
Psilocybe_strictipes_WTU-F-011411	*Psilocybe strictipes*	***Phaeonematoloma* sp.**	Washington, USA	N/A	1974	WTU	WTU-F-011411

Psilocybe_subcoprophila_UBC-F977	*Psilocybe subcoprophila*	***Deconica subcoprophila* (Britzelm.) E. Horak**	British Columbia, Canada	N/A	1984	UBC	UBC-F977
Psilocybe_subpsilocybioides_HOLOTYPE_CFMR-PR-5684	*Psilocybe subpsilocybioides*	***Deconica subpsilocybioides* (Guzmán, Lodge & S.A. Cantrell) Bradshaw, Ram.-Cruz & Dentinger, comb. nov.**	Puerto Rico	Holotype	1999	CFMR	CFMR-PR-5689
Psilocybe_subviscida_VPI-F-0003697	*Psilocybe subviscida*	***Deconica subviscida* Peck**	Virginia, USA	N/A	1983	VPI	VPI-F-0003697
Psilocybe_tuberosa_WTU-F-011378	*Psilocybe tuberosa*	***Strophariaceae***	Washington, USA	N/A	1989	WTU	WTU-F-011378
Pluteus_salicinus-KM-pgler-1679	*Pluteus salicinus*	***Pluteus salicinus* (Pers.) P. Kumm.**	Netherlands	N/A	1970	KM	K-M 265162
Pluteus_albostipitatus_KM-54312	*Pluteus albostipitatus*	***Pluteus albostipitatus* (Dennis) Singer**	Trinidad	N/A	1949	KM	KM-54312
Gymnopilus_luteofolius_KM-27062	*Gymnopilus luteofolius*	***Gymnopilus luteofolius* (Peck) Singer**	Missing	N/A	Missing	KM	KM-27062
Psilocybe_washingtonensis_WTU-F-055019	*Psilocybe washington*	**Unidentifiable**	Oregon, USA	N/A	1986	WTU	WTU-F-055019


A
B
C
D
E
F
G
H

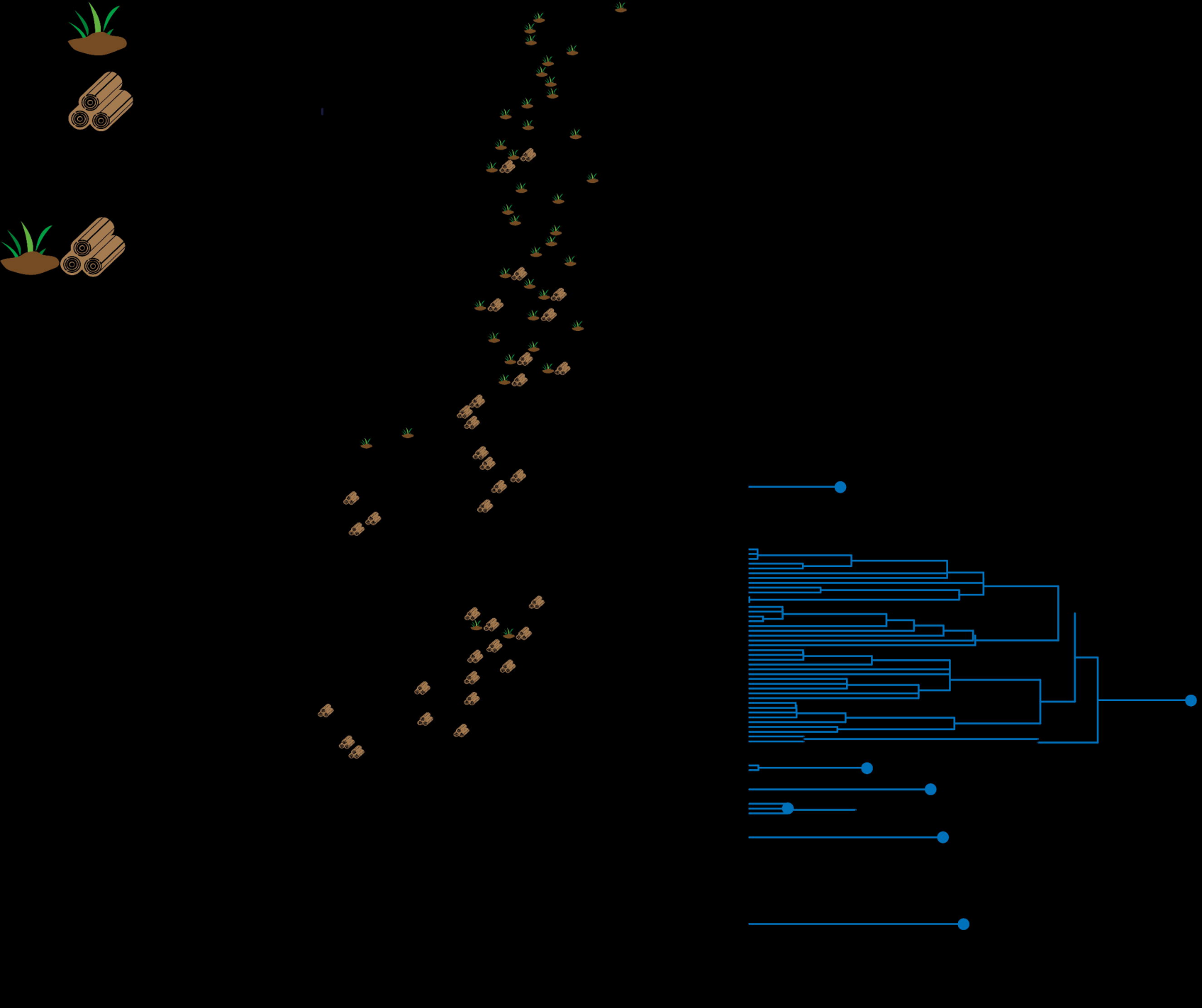

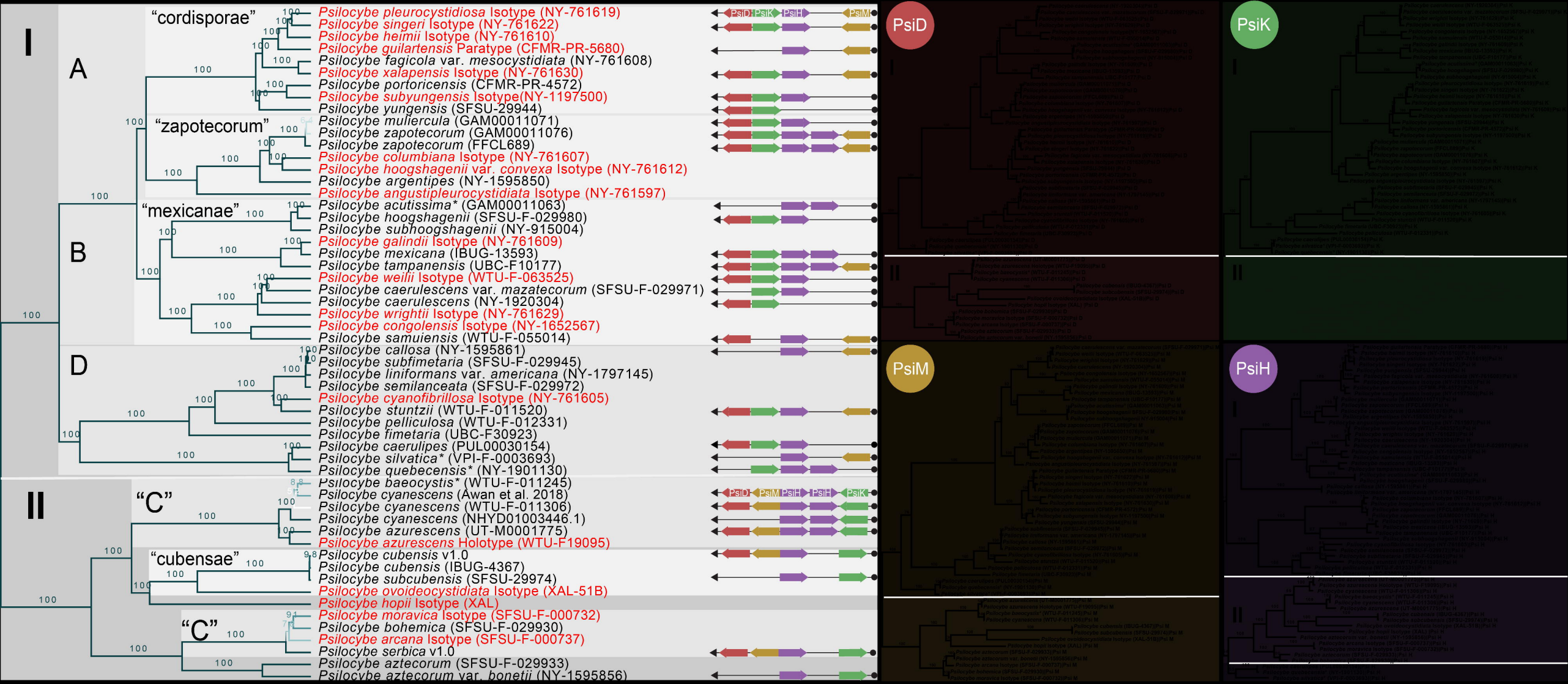
I
A
B
D
II
"C"
"cubensae"
"C"
"cordisporae"
"zapotecorum"
"mexicanae"
Psilocybe pleurocystidiosa Isotype (NY-761619)
Psilocybe singeri Isotype (NY-761622)
Psilocybe heimii Isotype (NY-761610)
Psilocybe guilartensis Paratype (CFMR-PR-5680)
Psilocybe fagicola var. mesocystidiata (NY-761608)
Psilocybe xalapensis Isotype (NY-761630)
Psilocybe portoricensis (CFMR-PR-4572)
Psilocybe subyungensis Isotype(NY-1197500)
Psilocybe yungensis (SFSU-29944)
Psilocybe muliercula (GAM00011071)
Psilocybe zapotecorum (GAM00011076)
Psilocybe zapotecorum (FFCL689)
Psilocybe columbiana Isotype (NY-761607)
Psilocybe hoogshagenii var. convexa Isotype (NY-761612)
Psilocybe argentipes (NY-1595850)
Psilocybe angustipleurocystidiata Isotype (NY-761597)
Psilocybe acutissima* (GAM00011063)
Psilocybe hoogshagenii (SFSU-F-029980)
Psilocybe subhoogshagenii (NY-915004)
Psilocybe galindii Isotype (NY-761609)
Psilocybe mexicana (IBUG-13593)
Psilocybe tampanensis (UBC-F10177)
Psilocybe weilii Isotype (WTU-F-063525)
Psilocybe caerulescens var. mazatecorum (SFSU-F-029971)
Psilocybe caerulescens (NY-1920304)
Psilocybe wrightii Isotype (NY-761629)
Psilocybe congolensis Isotype (NY-1652567)
Psilocybe samuiensis (WTU-F-055014)
Psilocybe callosa (NY-1595861)
Psilocybe subfimetaria (SFSU-F-029945)
Psilocybe liniformans var. americana (NY-1797145)
Psilocybe semilanceata (SFSU-F-029972)
Psilocybe cyanofibrillosa Isotype (NY-761605)
Psilocybe stuntzii (WTU-F-011520)
Psilocybe pelliculosa (WTU-F-012331)
Psilocybe fimetaria (UBC-F30923)
Psilocybe caerulipes (PUL00030154)
Psilocybe silvatica* (VPI-F-0003693)
Psilocybe quebecensis* (NY-1901130)
Psilocybe baeocystis* (WTU-F-011245)
Psilocybe cyanescens (Awan et al. 2018)
Psilocybe cyanescens (WTU-F-011306)
Psilocybe cyanescens (NHYD01003446.1)
Psilocybe azurescens (UT-M0001775)
Psilocybe azurescens Holotype (WTU-F19095)
Psilocybe cubensis v1.0
Psilocybe cubensis (IBUG-4367)
Psilocybe subcubensis (SFSU-29974)
Psilocybe ovoideocystidiata Isotype (XAL-51B)
Psilocybe hopii Isotype (XAL)
Psilocybe moravica Isotype (SFSU-F-000732)
Psilocybe bohemica (SFSU-F-029930)
Psilocybe arcana Isotype (SFSU-F-000737)
Psilocybe serbica v1.0
Psilocybe aztecorum (SFSU-F-029933)
Psilocybe aztecorum var. bonetii (NY-1595856)
PsiD
PsiK
PsiM
PsiH